Prediction of Added resistance in waves

Numerical method with an experimental setup

Vinodh Pichumani

Technische Universiteit Delft

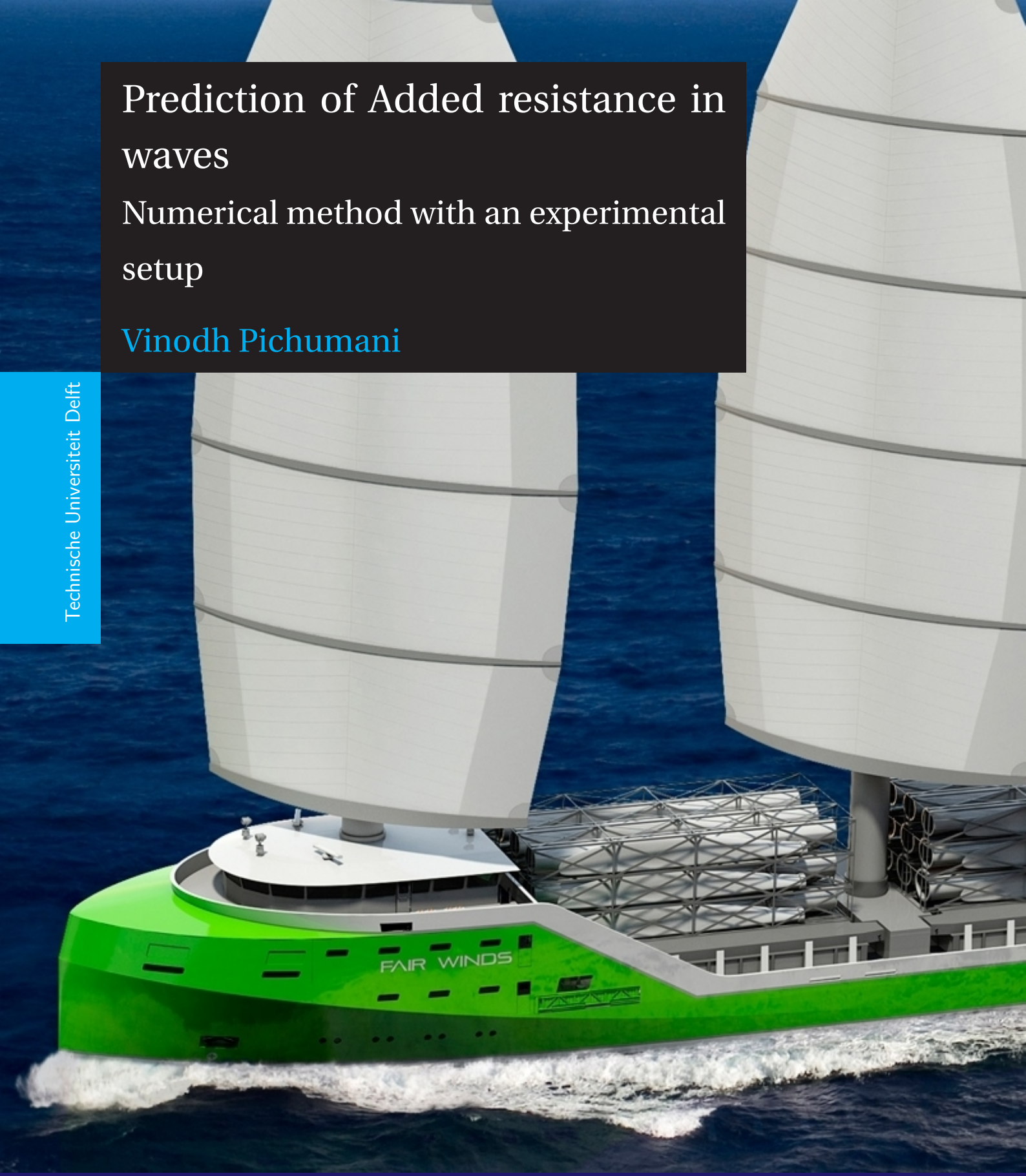

TU Delft Delft University of Technology

Challenge the future

PREDICTION OF ADDED RESISTANCE IN WAVES

NUMERICAL METHOD WITH AN EXPERIMENTAL SETUP

by

Vinodh Pichumani

in partial fulfillment of the requirements for the degree of

Master of Science
in Offshore and Dredging Engineering

at the Delft University of Technology,
30 October 2017

Student number:	4422724	
Supervisor:	Prof. dr. ir. R.H.M Huijsmans	
	Ir. Nico van der Kolk	
Thesis committee:	Prof. dr. ir. S.A Miedema,	TU Delft

An electronic version of this thesis is available at http://repository.tudelft.nl/.

TU Delft Delft University of Technology

ABSTRACT

The shipping industry constantly strives to improve – allowing productivity and sustainability to be tapped in the best possible way. The concept of sail-assisted propulsion of modern ships is a major step in that direction. It basically adds the natural advantage of direction-dependent wind force to the conventional primary drive in the form of a diesel engine. The idea of using sails and natural wind as a means of transport is richly derived from maritime history. An effective combination with modern technology would massively help in economic ship transportation with largely reduced carbon footprints.
This thesis is a step closer to that goal. The focus here is to describe the added wave resistance acting on a sail-assisted ship model, Ecoliner. There are two major technical aspects to this general situation:

1. description of the hydrostatic stability and response of sails to winds and,
2. the hydrodynamic investigation of loads effects on the hull

Point 2 is the obvious focus of attention in this work. This thesis is a follow-up of an experiment done at TU Delft, November 2013 to determine the influence of heel and leeway on added wave resistance on the said ship model.
Diffraction method based numerical analyses have been carried out to establish the added resistance for three different ship heel angles and three leeway angles over two different sailing speeds. Validation of the performed experiment is done as well as new findings regarding the sensitivity of the model variables are reported.
The highest leeway angle of 9 degrees, in particular, is seen to have a significant effect in the increasing the added resistance. This effect was previously not captured by experiments and helps give an overview on which parameters the Ecoliner ship's performance is more sensitive to. Effect of constraining or allowing roll is also found to be an especially important parameter. The margin of difference between analysis and experiment results improves by about 20 to 25% after a proper analysis of roll hydrodynamics and putting that factor in.
This work will hopefully be a stepping stone in further research endeavours in this field concerning optimizing Ecoliner as an end market product. Recommendations are given in this report for specific follow-up work in both the analytical as well as the experimental domain for the hull-related study.

ACKNOWLEDGEMENT

This report is a reflection of the work done during my graduation thesis, in partial requirement for my Master of Science degree in Offshore and Dredging Engineering, at Delft University of Technology. Damen Shipyards group is the sponsor of my thesis study and their support is gratefully acknowledged.

First of all, I would like to thank my supervisor, Ir. Nico van der Kolk, who guided me through every step of the way, and was always available to answer my questions. He instilled the knowledge and the thought process in me, which is what led to the successful completion of this thesis study. I wholeheartedly thank him for his cooperation and support. I would like to thank Prof. dr. ir. R.H.M. Huijsmans for his guidance and motivation for the thesis. He also provided me with valuable insights into the practical aspects related to my study.

Apart from people in TU Delft, I would like to thank Ir. Anand Sreedharan, Ir. Satish Prabhakar and Ir. Raghu Krishnan for their support and sharing their knowledge in the field of hydromechanics. I would also like to extend my gratitude to Er. Jayaprakash Krishnasamy who mentored me through the hardest of times.

I would like to thank all my colleagues and friends from the university especially Ratnakar Gadi, for all the memorable moments during my journey in becoming a master student.

Finally, I dedicate this work to my dear parents for their unconditional and unwavering support behind my studies and for providing me with the best of everything in my life.

Vinodh Pichumani,

Delft, The Netherlands.

October 2017.

CONTENTS

List of Figures

List of symbols and Abbreviation

β	Leeway angle
λ	wave length
∇	Displacement
ω	Wave frequency
ω_e	Encounter frequency
ϕ	Roll motion
ρ	Density of water
θ	Pitch motion
φ_d	Diffraction potential
φ_I	Incident wave potential
$\vec{X}$	Collocation point
ζ	Wave amplitude
F_D	Diffraction force
F_{fk}	Froude Krilov force
K_{xx}	Radii of gyration alon X- axis
$R_{aw_{nd}}$	Non-dimensional added resistance
R_{aw}	Added resistance of waves
B	Breadth of the model
COG	Center of gravity
fn	Froude number

G	Green's function
g	acceleration due to gravity
k	wave number
L	Length of the model
RAO	Response amplitude Operator
x	Surge motion
y	Sway motion
z	Heave motion

1

INTRODUCTION

This section gives an overview of the sail assisted vessel Ecoliner, the scope of this research to predict the added resistance with the help of numerical tool and to validate the results with data from a previous experiment. The method followed to acquire this objective is explained briefly in the subsequent sections.

1.1. DAMEN SHIPYARDS

This Master thesis is funded by Damen Shipyards Group. It was established in the year 1927 by Jan and Marinus Damen. Damen is one of the largest shipbuilding companies which has 32 shipyards worldwide. It has a wide product range including tug boats and work boats, offshore vessels, high speed crafts and so on. In recent years, Damen has been interested in exploring sustainable and economical ways of operating offshore vessels.The LPNG tanker, Ecoliner is a result of these efforts and it uses the concept of a sail assisted ship.

1.2. SAIL ASSISTED SHIP

Modern ship are driven by motors which consume enormous amount of fuel in order to propel the ship. So, there will be constant supply of fuel to the engine. This magnitude increase in proportion to the dead weight (displacement of laden ship) and as such, is a more relevant factor as the industry moves towards bigger ships. For an quite number of decades the oil price is fluctuating and one cannot rely on this volatile price. An alternative measure has made by the shipping industry which is sail assisted or wind assisted ship. In addition to the economic advantages of less fuel consumption, such a method leaves way less carbon footprint.

It is an optimal way of combining a non-renewable energy source (i.e diesel fuel) with a natural and renewable source like wind to yield positive results. With increased shipping world over, a reduction in fuel emissions is highly beneficial not just for short-term economics but also for the sustained future of the planet. The key idea of sail assisted ship is to use the wind as an auxiliary power source in addition to the primary diesel engine system in the moderate sea condition.

To improve the energy conservation and reduce emissions, this concept of sailing is developing rapidly among the industry. Various studies have been carried out to find the application of this concept and one of the research [4] proposed that about 50% of propulsive power can be acquired by ocean wind power. And K.Ouchi also stated that through this, the operational cost can be reduced upto 22 percent in comparison to the conventional 100 percent fuel-based ships.

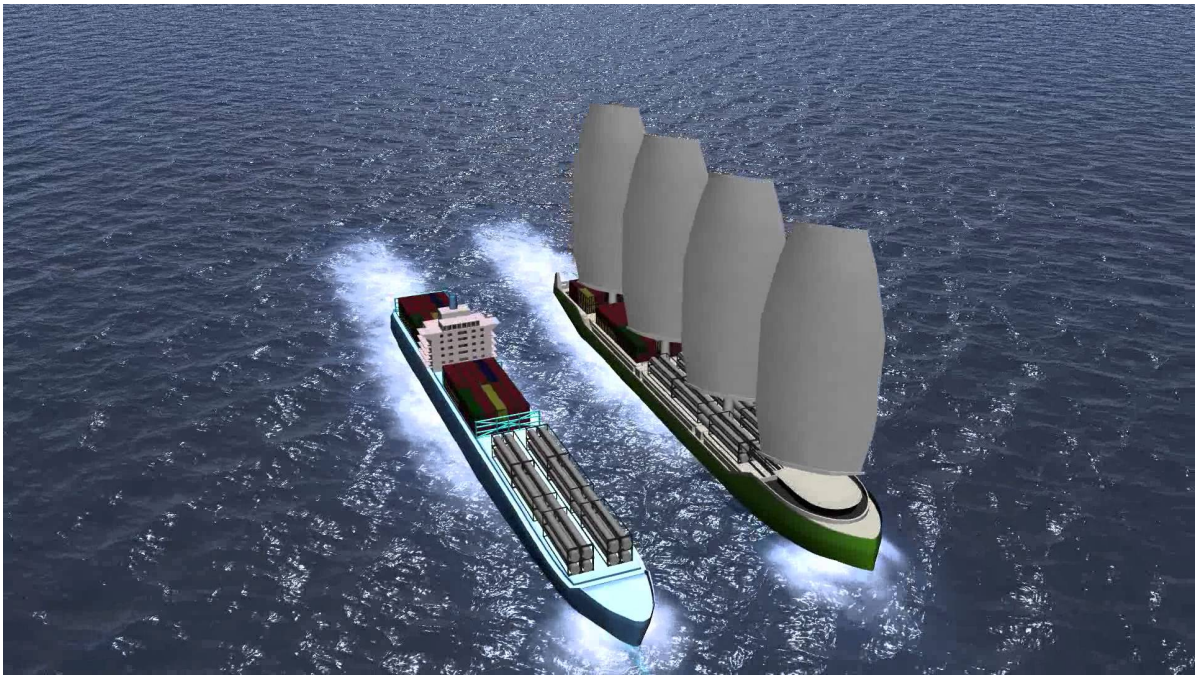

Figure 1.1: Comparison of conventional ship and eco liner

1.3. PROBLEM BACKGROUND

In the past, ship optimization was done for calm water conditions, trial voyages were carried out in benign seas. But the ship is designed for the operational conditions where they need to encounter the waves. This brings the importance of added resistance which helps in improving ship speed because when the ship navigates in the actual sea, the ship's forward speed is decreased due to added resistance [5].

On the other hand International Maritime Organization (IMO) has decided to investigate the Energy Efficiency Design Index to control the emission of green house gases from the ships. This brings the added resistance problem into the spot light for the optimum hull design and to reduce the resistance experienced by the ships. Therefore accurate prediction of added resistance is important. Many effort was put into predicting added resistance by conducting experiments and several methods were introduced in the past. Among these methods, Salvesen method was chosen for this research which will be explained in up coming chapter. Due to the action of wind and waves, Ecoliner has different characteristics compare to conventional vessel like maintaining the stability of the vessel is one of the major considerations in wind assisted ship [6]. In this research heel and leeway condition are considered as the changes in course direction of the ship and the added resistance is predicted in these two conditions.

1.4. OBJECTIVE

- To predict added resistance under the influence of heel and leeway conditions for given forward speed.
- Validation of numerical results with the previous experimental data and proposing a new experimental setup to increase the experimental accuracy.

1.5. STRUCTURE OF THE THESIS

In chapter 2 a theoretical background required for this research, such as types of for predicting added resistance and the difference in the computational technique of Seaway or Octopus Office and ANSYS AQWA and the chosen method for finding added resistance are explained.

In chapter 3 the comparison between the two numerical tools (Seaway and ANSYS AQWA) was done and from that suitable software is chosen.

In chapter 4, the added resistance is predicted using Salvesen method for heel and leeway condition with different speeds. The required hydrodynamic coefficients are extracted from ANSYS AQWA and the post processing is done using MATLAB.

In chapter 5, the results obtained from chapter 4 are validated with experimental data of added resistance which was provided by TU Delft. After the comparison, a experimental setup was proposed in order to increase the experimental accuracy.

2

THEORETICAL BACKGROUND

2.1. INTRODUCTION

In this chapter, we discuss about the basic definitions and theoretical background that is required for finding added resistance. In the first part, we discuss about the axis definitions of ship and through this positions of the scaled model are established. Further sections deal with different theories of finding added resistance and a short motivation for the chosen theory.

2.2. AXIS DEFINITIONS

Based on the right handed co-ordinate system, there are three types of axis system:

EARTH FIXED COORDINATES

In this axis system $x_0 y_0 z_0$ has a origin (S) based on the mean still water. The positive x_0 direction depends on the wave propagation,, y_0 is in the portside and z_0 is positive upward.

BODY BOUND COORDINATES

In this system the origin is defined at centre of gravity (G) of the body and based on this origin the positive x_b in the propagation direction of the ship and y_b is in the port-side and z_b is positive upward.

STEADY TRANSLATING

If the ship moves at a constant speed V, normally in this case the analysis are carried out based on this co-ordinate system. In mean position the body bounded co-ordinates $G(x_b, y_b, z_b)$ and steady translating axis $O(x, y, z)$ will be considered as the same axis.

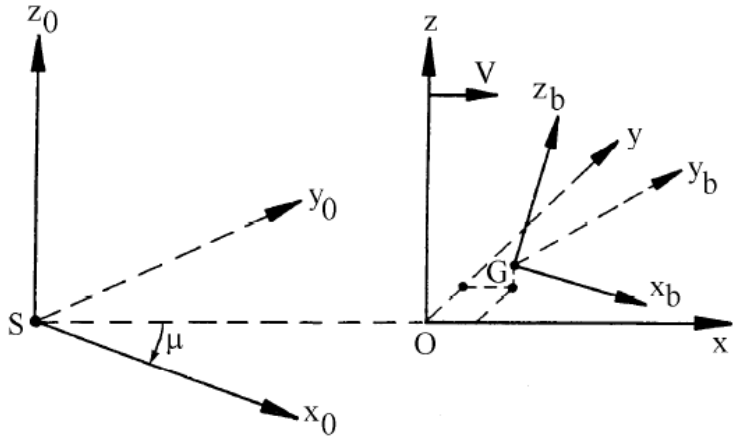

Figure 2.1: Axis definitions

For the background experiment [7], based on the nature of setup, raw results were in the body bound coordinate system. The researcher further transformed them to the earth fixed coordinates and compared with his numerical results. All analysis results within this thesis are reported in the earth fixed coordinate system to enable a consistent comparison.

2.3. SHIP MOTIONS

The three translational motions about X-, Y- and Z- axes respectively are surge, sway and heave. The corresponding rotational motions are roll (ϕ), pitch (θ) and yaw (ψ).

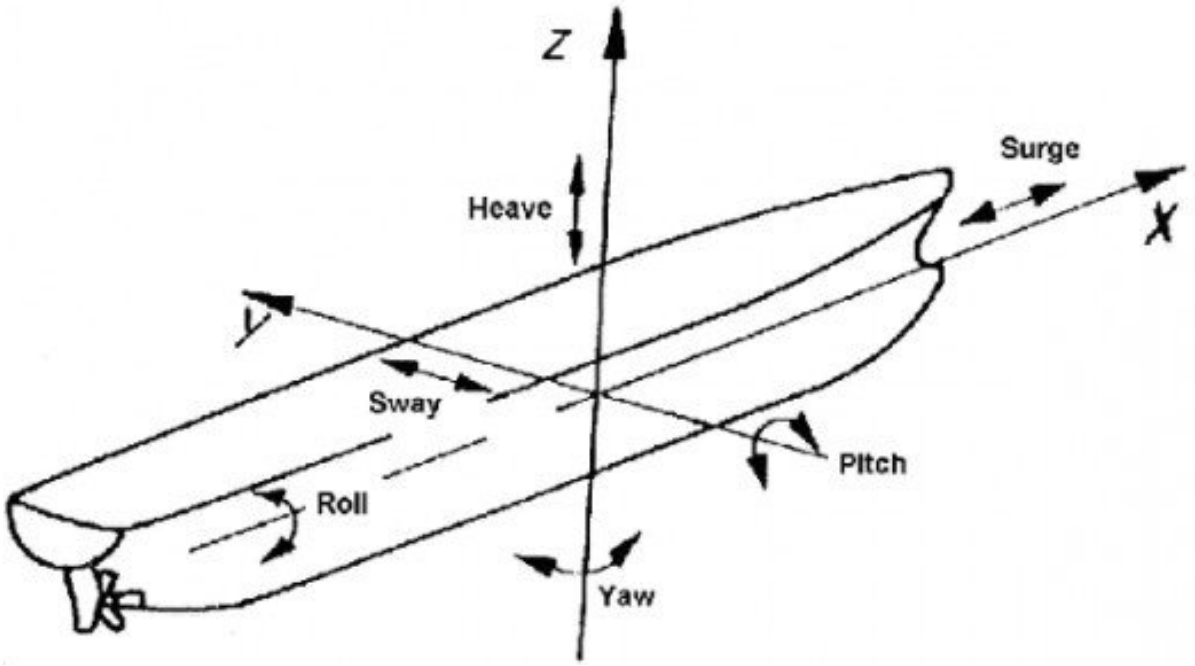

Figure 2.2: Six degree of freedom [1]

For geometric orientation, all the axes are defined relative to a coordinate system with:

Origin x=0 at APP (Aft Perpendicular) - positive x-axis pointing to bow
Origin y=0 at CL (Centreline) - positive y-axis pointing to portside
Origin z=0 at BL (Baseline) - positive z-axis pointing upward

The static angular offsets in the three axes may be understood as heel, trim and leeway respectively.

2.4. ORIENTATION

2.4.1. HEEL

Heel is defined as the inclination of the ship with respect to bounded axis (x_b) caused by the the static current or wave force or under wind pressure on the body. In simple it can also be termed as roll in static mode. This heel condition generates asymmetric water plane on the hull which makes the analysis more computationally intensive.

2.4.2. LEEWAY

Leeway is defined as the drift of the ship from its course direction towards lateral side caused by the effect of the wind on the ship. In simple it is also known as the static yaw angle by considering x_b with respect to x_o. In this case the water plane area is considered to be symmetric but the pressure distribution around the hull is not symmetric due to the

angle of attack.

2.5. WAVE FIELD

Mathematically modeling the exact ocean waves is not feasible, because the real waves are composed of different frequencies. Further, there is interaction of wave components from different directions. Wave trains in nature, are thus, frequency and direction dispersed, making precise modeling very challenging. To overcome this, many simplified theories are stated in different literature such as linear wave theory, higher order Stokes wave theory and irregular waves (based on the spectra).

Among above mentioned theory, the most efficient and popularly used one is small amplitude linear wave theory because first order regular waves are taken into account which makes the computation less tedious. The important concept introduced in the linear theory is dispersion relationship [8], derived from the kinematic and dynamic boundary condition. The general relationship for arbitrary water depth is

$$\omega^2 = gktanh(kh) \tag{2.1}$$

But in this research, only deep water ($h \rightarrow \infty$) condition is used for the computation which brings to a simplified equation

$$\omega^2 = gk \tag{2.2}$$

The waves can be classified into long waves, intermediate waves and short waves based on the ratio of length of the ship to wavelength [9] ($\lambda = 2 * \pi / k$).

Ratio	Type of wave
$\lambda/L \leq 0.3$	Short waves
$0.3 \leq \lambda/L \leq 1$	Intermediate waves
$\lambda/L \geq 1$	Long waves

Table 2.1: Classification of waves

2.6. FREQUENCY DOMAIN

In frequency domain, the waves are regular and harmonic which makes ship motion problems relatively easy to describe and can be solved in less computational effort. The mathematical description of motions in such a setup are achieved by super position of different wave frequency. In this research, the frequency domain analysis is performed by the Octopus Office or Seaway and ANSYS AQWA. Later, by comparing these two numerical tools suitable one is chosen for the analysis. Linearized condition can be explained as shown in the figure 2.3 ,the given wave spectrum is harmonic wave and the response of the ship is also harmonic. In simple the output should be equal to the input. Hence in the frequency domain analysis are performed in the linearised condition.

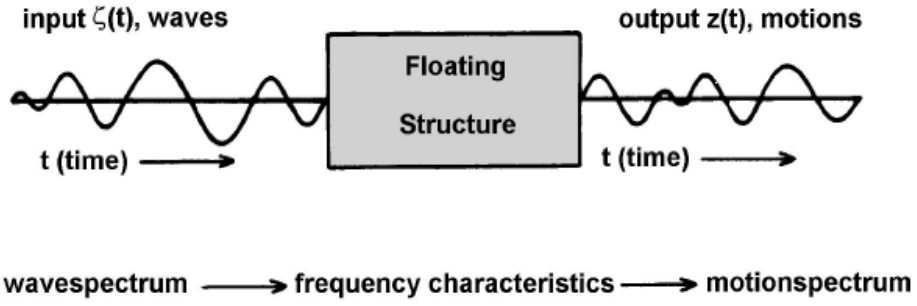

Figure 2.3: Linearization [2]

2.7. ADDED RESISTANCE

The added resistance is a speed dependent component. It can be defined as the extra resistance encountered when the ship moves at a constant forward speed in presence of waves compared to motion in calm seas. This is due to dissipation of energy which is caused by the waves generated by the ship and as well the reflection of incident waves. In moderate sea conditions when ship travels below the design speed about 50% of its total resistance is caused by the added resistance [3]. This shows the importance of added resistance in the design of high speed craft.

$$R_{aw} = \text{Mean total resistance - Calm water resistance}$$

In general, the added resistance is predicted from the sum of the motion and reflection induced component [9]. Motion induced components and the reflection induced component are high when the wave length to ship length ratio is equal to one. But in the long

waves influence of both component is negligible, and in short waves reflection component is the dominant component [10]. This research deals with ship facing the head waves, heave and pitch motions have major influence on the added resistance when its in upright condition. But when the ship is in heel or leeway condition the influence of roll motion also plays a role in prediction of R_{aw} which can be seen in the upcoming results. Based on above mentioned factors, the added resistance can be calculated numerically by various methods but in this research, Salvesen method is used and this method is explained in section 2.9. The frequency domain is employed for estimating the added resistance and thus all non-linearities are neglected.

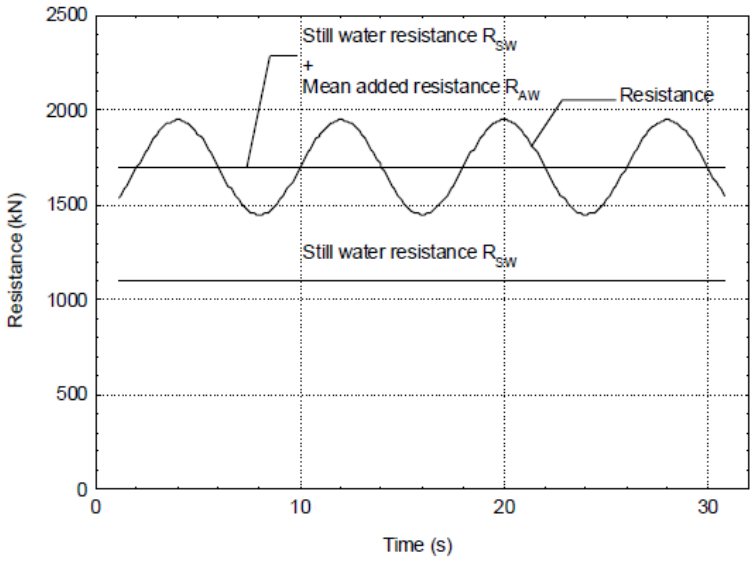

Figure 2.4: Added resistance in waves [2]

2.8. COMPONENTS OF ADDED RESISTANCE

The components that attributed to added resistance are three parts which are given as:

- The interference between the incident wave systems and the waves that are the results of the ship heave and pitching. This is the combined radiation (body motion) and incoming wave loads.
- A component due to wave systems experiencing some wave reflection from the ship. This is often only of importance when the wavelengths are small compared to the ship length. This force is due to the reflected/ scattered wave component. The incoming and the reflected wave together form the diffraction force component.
- An additional mass and a force that is due to the damping force from the heaving and pitching motions of the vessels when the water is calm. This is the radiation component of the force.

From the figure 2.5, it can be seen that the high frequencies range are induced by the diffraction and lower frequencies are induced by radiation components. Because of the influence of both radiation and diffraction components, the transition region needed to be focused in particular [5]. It's evident that the peak of the added resistance can be found in this region.

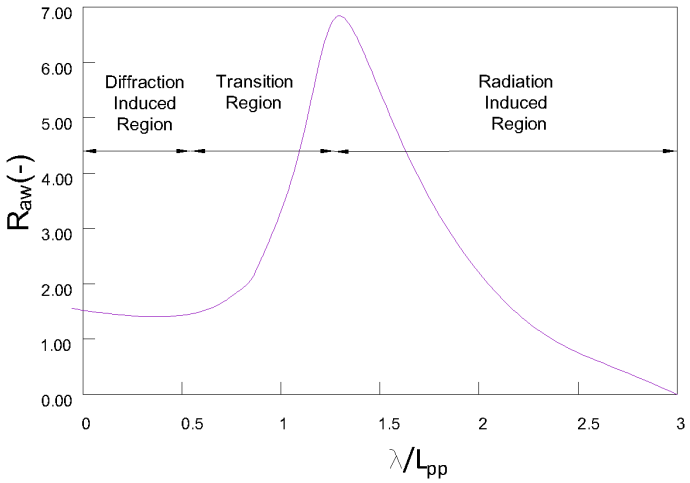

Figure 2.5: Added resistance components

INFLUENCE OF WAVE CHARACTERISTICS ON ADDED RESISTANCE

- Wave length
- Wave height
- Wave encounter frequency
- Wave heading

INFLUENCE OF WAVELENGTH

Added resistance is influenced by the relative vertical motion. The relative vertical motions are the pitch and heave motions. These relative vertical motions are mainly dependant on the wave length and also geometry of the ship plays a role. It can be seen that the added resistance reaches its maximum value when the ratio of the wavelength to the ship length is one. Against long waves the added resistance approaches zero because the wave and ship motions are in phase. On the other hand added resistance in short waves is small. This influence is explained in detail in section 4.3.

INFLUENCE OF WAVE HEIGHT

In real scenario, as the wave height increases, there will be increase in the wetted surface area of the hull and as a result pressure around the hull as well increases. Most of the numerical tools use pressure distribution around the hull to find the hydrodynamic coefficients and these coefficients are used in predicting the added resistance. The significance of the wave height can be understood from the definition of added resistance in terms of first order approximation where the added resistance is proportional to the square of the wave height [11]. However, in this study regular waves are used, which means there will be no change in the wave height in the entire numerical analysis.

INFLUENCE OF ENCOUNTER FREQUENCY

As mentioned in the previous section, the term added resistance is used to determine the speed loss which clearly shows the importance of forward speed. When the ship moves with forward speed, it experiences encounter frequency (ω_e) instead of wave frequency (ω). If the ship moves with increasing forward speed against the waves, the encounter frequency experienced by the ship also increases which in turn increases the added resistance.

INFLUENCE OF WAVE HEADING

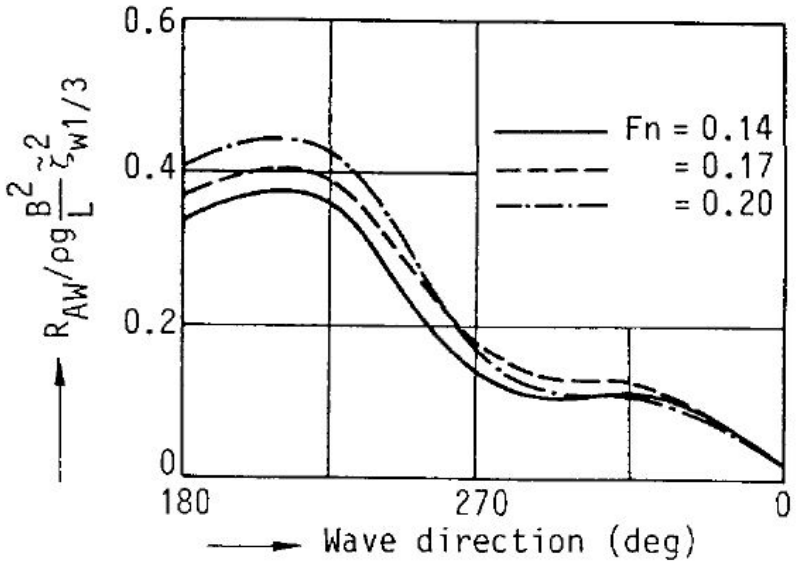

Figure 2.6: Influence of wave direction [3]

It can be seen that as the wave moves from head waves (180^o) to following waves ($0)^o$, added resistance gradually decreases. And the added resistance is maximum when the wave heading is 180^o even for different speeds.

2.9. SALVESEN METHOD

When ship travels in sea, it encounters incoming waves which produces time varying force on the body. Even if the mean of incoming waves is zero, mean value of the force is not zero due to quadratic effects. This effect is responsible for an extra load on the ship called added resistance and this leads to a power loss.

The added resistance can be predicted in few ways like Momentum and Energy conversation method, radiated energy method and direct pressure integration methods. The most popularly used methods are radiated energy method and direct pressure integration method which gives satisfactory results in short time. In previous thesis [7] added resistance was estimated from Gerritsma Beukelman method [12] which is based on the radiated energy method.

$$P = \int_0^{T_e} \int_L \left(N_{33}^{'} - V \frac{dM_{33}^{'}}{dx_b} \right) V_z^{*2} dx_b dt \tag{2.3}$$

From the above equation 2.3, he defined the wave energy radiated during one period of oscillation of a ship in regular waves and the added resistance is calculated as:

$$\frac{R_{aw}}{\zeta_a^2} = \frac{-kcos\mu}{2\omega_e} \int_L \left(N_{33}^{'} - V \frac{dM_{33}^{'}}{dx_b} \right) \left(\frac{V_z^*}{\zeta_a} \right)^2 \tag{2.4}$$

This was first developed for head waves and after few years, Salvesen (1978) used Gerritsma Beukelman method and extended his method (GB) to predict added resistance for oblique waves but by using potential flow solution[13].

The reason this method is used in this research is because of the flexibility to take the diffraction component into account separately in the computation of added resistance as given in the equation 2.5. It is true that that the added resistance is a second order phenomenon but it can be determined from the first order heave and pitch motions calculated in the diffraction suite ANSYS AQWA.

Advantage over the original method that Salvesen employed (strip theory) is more precise description of the wave diffraction problem within the 3-D potential theory framework. Back then in the 1970s, lack of computing power to carry out 3-D hydrodynamic calculations was a definite reality. In this entire thesis however, ANSYS AQWA results are used for

the comparisons and to draw scientific conclusions.

$$R_{aw} = -\frac{i}{2} k \cos\beta \sum_{j=3,5} \zeta_j \left\{ (F_j^I)^* + F_j^D \right\} + R_7 \tag{2.5}$$

where ζ_j is the motion of ship in heave and pitch. Froude-Krylov force F_j^{I*} and diffraction force F_j^D are complex conjugate terms. The complex conjugate terms are predicted from their respective phase angle by using Euler's method.

$$F_{j_{3,5}} e^{\left(i\omega t+\phi\right)} = F_{j_{3,5}} \Big((\cos\omega t + \phi) + i(\sin\omega t + \phi) \Big)$$

In the frequency domain force can now be defined in terms of the force amplitude F_{jK} and phase ϕ and Salvesen method is based on the linearized condition as well

$$R_7 = -\frac{1}{2} \zeta_1^2 \frac{\omega^2}{\omega_e} k \cos\beta \int_L e^{-2kds} \left(b_{33} + b_{22} \sin^2\beta \right) dx \tag{2.6}$$

where, ζ_j is the incident wave amplitude, d is the sectional draft and s is the sectional area- coefficient of the single strip. b_{33} and b_{22} are the sectional heave and sway damping coefficient respectively.

This R_7 is called as radiation damping and its predicted from Seaway in order to reduce the computation time because ANSYS AQWA uses panel method and finding the sectional component for each panel will be tedious.

COMPUTATIONAL METHOD

2.10. STRIP THEORY

The strip theory considers that the ship is sliced into number of finite transverse parts, connected to each other in a rigid way. The hydro dynamical analysis is done by considering each strip as a part of an infinitely long cylinder as shown in figure 2.7. This approach largely takes away the interaction between individual strips; effectively reducing each dissected plane (strip) to a two-dimensionsal potential source. This assumption some times neglect the waves generated by the fore and aft which is called end effects [14].

The strip theory computational method is applicable only if the following conditions

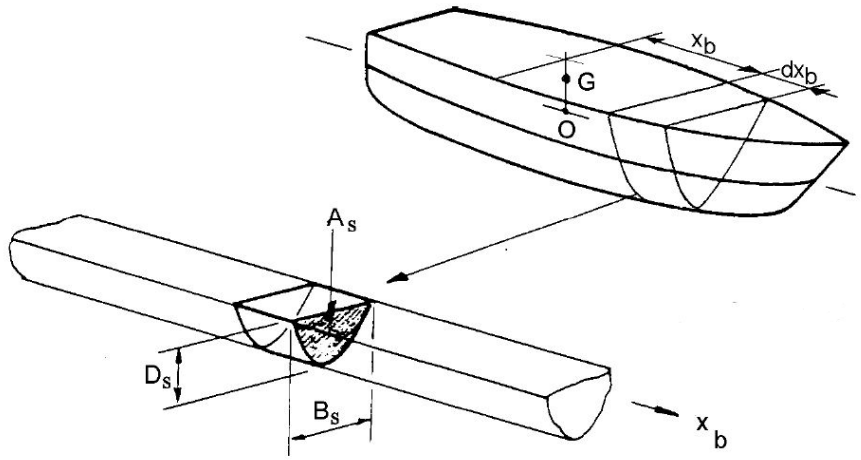

Figure 2.7: Assumption of strip theory

are satisfied [14].

- The body is assumed to be rigid and floating in ideal fluid. An ideal fluid in this context means non-viscous, incompressible and irrotational.
- Long, slender bodies, about L/B >=3 indicated by experiments, may be calculated using strip theory. In other words the ship is so long relative to an individual discretized strips that adjacent strip do not feel each other.

After satisfying above mentioned conditions, the seaway can compute the required hydro-mechanical co-efficient in zero forward speed and forward speed. It is pointed out that by thus describing the flow problem, it is linearized and the strips are connected to each other in rigid manner so that 3-D interaction effects can be taken away.

ZERO FORWARD SPEED

The strip theory is a 2-D theory which means the 3-D loads are obtained by integrating 2-D loads. However the strip theory uses simple approach to compute the six degree of motions but finding the surge hydrodynamic coefficient is not easy because of assumption that each section is considered to be the infinitely long cylinder as shown in figure 2.7 that makes the calculation complex. But 2-D surge hydrodynamic coefficient is determined from 2-D sway coefficients and these values are transferred as surge coefficients using a empirical methods which is based on the three dimensional calculation. Its found that influence of surge is not much in head waves and hence its neglected. The values of pitch and yaw moments are obtained from the 2-D values of heave and sway forces as given the equations:

$$X_{h1} = \int_L X'_{h1} \cdot dx_b \tag{2.7}$$
$$X_{h2} = \int_L X'_{h2} \cdot dx_b \tag{2.8}$$
$$X_{h3} = \int_L X'_{h3} \cdot dx_b \tag{2.9}$$
$$X_{h4} = \int_L X'_{h4} \cdot dx_b \tag{2.10}$$
$$X_{h5} = -\int_L X'_{h3} \cdot x_b \cdot dx_b \tag{2.11}$$
$$X_{h6} = \int_L X'_{h2} \cdot x_b \cdot dx_b \tag{2.12}$$

X_{hj} is the sectional hydro mechanical force or moment in the j th direction. The same equation is followed for the wave exciting force but a small change should be made instead of X_{hj} it should be represented as X_{hw}.

FORWARD SPEED

The main difference between zero forward speed and forward speed is difference in the influence of wave particle velocity. In the case of zero forward speed the excitation experienced by the body is based on the wave frequency where as in the forward speed condition, its based on the encounter frequency. This gives the variation in calculating the potentials but in both cases potential from the earth fixed coordinates system $\Phi(x_0, y_0, z_0)$(wave loads) is translated to steadily translating coordinates $\Phi(x, y, z)$ along with the speed of the vessel V. Two different types of strip theory methods are used in seaway.

1. **Ordinary Strip theory method**
2. **Modified strip theory method**

ORDINARY STRIP THEORY METHOD

According to literature [14], this is the first formulation method for finding the uncoupled hydro mechanical loads and wave loads in any direction which are given by.

$$X^*_{hj} = \frac{D}{dt}\left\{M'_{jj} \cdot \zeta^*_{hj}\right\} + N'_{jj} \cdot \zeta^*_{hj} + X'_{rs_j} \tag{2.13}$$
$$X^*_{\omega j} = \frac{D}{dt}\left\{M'_{jj} \cdot \zeta^*_{\omega j}\right\} + N'_{jj} \cdot \zeta^*_{\omega j} + X'_{fk_j} \tag{2.14}$$

However, in the forward speed case the results obtained using this method is said to be more or less intuitive which leads to the another method which is given below.

MODIFIED STRIP THEORY

This is the continuation of ordinary strip theory which was proposed by Tasai and the difference is that this includes the speed dependent part (ω_e) for computation of the hydro dynamic forces. This modified method is called as modified strip theory.

$$X^*_{hj} = \frac{D}{dt}\left\{\left(M'_{jj} - \frac{i}{\omega_e}N'_{jj}\right)\cdot\zeta^*_{hj}\right\} + X'_{rs_j} \tag{2.15}$$

$$X^*_{\omega j} = \frac{D}{dt}\left\{\left(M'_{jj} - \frac{i}{\omega_e}N'_{jj}\right)\cdot\zeta^*_{\omega j}\right\} + X'_{fk_j} \tag{2.16}$$

However, both the methods give the similar result, but in theoretical point of view modified strip theory suits well and in practical point of view ordinary strip theory matches with well with experimental data [15].

LIMITATIONS OF STRIP THEORY

Strip theory is used to compute the ship motion problem in short amount of time. This method depends on the symmetry of under-water hull and cannot solve the asymmetric water plane such as heel and leeway conditions. Since the focus of this thesis is on the sensitivity of added resistance to heel and leeway effects, it is considered a significant limitation. As a result, the strip theory is not considered as the chosen solution method.

2.11. PANEL METHOD

The strip theory is a simple way of solving the ship motion problem with adequate level of accuracy, depending on the problem at hand. After several years, advancement in technology and computation method leads to a method that can solve 3D problem. This method is called as the boundary element method or panel method. In panel methods the hull surface and free surface are divided into number of panels in all the three-dimensions and sources and dipoles are distributed constantly over each panel. Green's function by itself satisfies the Laplace equation.This method can be used for non-linear and linearised conditions but for this scope of research only linearised condition are used.

ZERO FORWARD SPEED APPROACH

VELOCITY POTENTIAL

SOURCE DISTRIBUTION METHOD

The velocity potential in ANSYS AQWA is space dependent term and its calculated using source distribution method. The source strength and potential in each panel are assumed

constant which is based on the principle of Hess-Smith constant panel method. The velocity potential is determined using source strength and they need to satisfy the following governing equation and boundary conditions.

LAPLACE EQUATION

$$\nabla^2\varphi = \frac{\partial^2\varphi}{\partial X^2} + \frac{\partial^2\varphi}{\partial Y^2} + \frac{\partial^2\varphi}{\partial Z^2} = 0 \tag{2.17}$$

LINEAR FREE SURFACE CONDITION

$$-\omega^2\varphi + g\frac{\partial\varphi}{\partial Z} = 0 \quad on \quad Z = 0 \tag{2.18}$$

BODY SURFACE EQUATION

$$\frac{\partial\varphi}{\partial n} = \begin{cases} -i\omega n_j & \text{for radiation potential} \\ \frac{\partial\varphi}{\partial n_j} & \text{for diffraction potential} \end{cases} \tag{2.19}$$

SEA BED SURFACE CONDITION

$$\frac{\partial\varphi}{\partial Z} = 0 \quad on \quad Z = -d \tag{2.20}$$

BERNOULLI EQUATION

$$p^(1) = i\omega\rho\varpi(\vec{X})e^{\{} - i\omega t\} \tag{2.21}$$

In frequency domain pulsating Green's function which satisfy above mentioned condition and the final equation is written as.

$$G\left(\vec{X},\vec{\xi},\omega\right) = \frac{1}{r} + \frac{1}{r_2} + \int_0^\infty \frac{2(k+v)e^{-kd}cosh\left[k(Z+d)\right]cosh\left[k(\zeta+d)\right]}{ksinh(kd) - vcosh(kd)} J_O\left(kR\right)dk + i2\pi\frac{2(k_0+v)e^{-k_0 d}cosh\left[k_0(Z+d)\right]cosh\left[k_0(\zeta+d)\right]}{sinh(k_0 d) + k_0 dcosh\left(k_0 d\right) - vdsinh\left(k_0\right)J_0\left(k_0 R\right)} \tag{2.22}$$

$$\Delta G(\vec{X},\vec{\xi},\omega) = \frac{\partial^2 G}{\partial X^2} + \frac{\partial^2 G}{\partial Y^2} + \frac{\partial^2 G}{\partial Z^2} = \delta\left(\vec{X} - \vec{\xi}\right) \tag{2.23}$$

With the help of Green's theorem, the velocity potential is expressed in simplified form by second kind Fredhol integral equation.

$$c\varphi(\vec{X}) = \int_{S_0} \left(\varphi\vec{\xi}\frac{\partial G(\vec{X},\vec{\xi},\vec{\omega})}{\partial n\vec{\xi}} - G(\vec{X},\vec{\xi},\vec{\omega})\frac{\partial\varphi\vec{\xi}}{\partial n\vec{\xi}}\right) \tag{2.24}$$

Then the source is introduced to above equation and the source strength is calculated by applying hull surface boundary condition. After many mathematical simplifications the velocity potential is determined as:

$$\varphi(\vec{X}) = \int_{S_0} \varphi\vec{\xi}\frac{\partial G(\vec{X},\vec{\xi},\vec{\omega})}{d}s \tag{2.25}$$

Once the velocity potential is found then the required hydrodynamic parameters are all obtained.

The equations 2.22 - **??** shows the importance of Green's function in finding the velocity potential and directly evaluating the frequency domain by Green's function in finite depth is time consuming because given Green's function satisfy the sea bed surface condition only at infinite depth. So ANSYS AQWA uses a Green's function database to efficiently calculate the Green's function and its first order derivative. The minimum frequency limit for this data base is given equation 2.26. However, in this research, the infinite water assumption is used.

$$\omega_{min} = 0.001\sqrt{\frac{g}{d}} \tag{2.26}$$

2.12. FORWARD SPEED CORRECTION

The entire computations in this thesis are done with the forward speed condition. In forward speed coordinates in the frame of reference differs from the zero forward speed condition because of the moving reference frame and its given as:

$$\vec{X} = \vec{U}t + \vec{x} \tag{2.27}$$

In forward speed instead of wave frequency, encounter frequency is used. This is determined as

$$\omega_e = \omega - \frac{\omega^2 U}{g}\cos\beta \tag{2.28}$$

LINEAR FREE SURFACE CONDITION

$$\left(-i\omega_e + \vec{U}.\nabla\right)^2 + g\frac{\partial\varphi}{\partial Z} = 0 \quad on \quad Z = 0 \tag{2.29}$$

BODY SURFACE CONDITION

$$\frac{\partial\varphi}{\partial n} = \begin{cases} -i\omega_e n_j + U m_j & \text{for radiation potential} \\ \frac{-\partial\varphi_I}{\partial n} & \text{for diffraction potential} \end{cases} \tag{2.30}$$

The term m in above equations are due to Taylor series expansion, which is due to linearisation of the interaction between steady translating body and its motions.

BERNOULLI EQUATION

The prediction of first order hydrodynamic pressure through Bernoulli equation also changes due to addition of forward speed term into the equation 2.31

$$p^{(1)} = \rho\left[i\omega_e\varphi(\vec{x}) + \vec{U}\cdot\nabla\varphi(\vec{x})\right]e^{-}i\omega_e t \tag{2.31}$$

Once the pressure was found then the step would be finding the forces. In this research Froude Krilov force and diffraction force are used and the way the these two forces predicted are explained below.

$$F_{Ij} = -\rho\int_{S_0}\left(i\omega_e\varphi(\vec{x}) + \vec{U}\cdot\nabla\varphi_I(\vec{x})\right)n_j ds \tag{2.32}$$

$$F_{dj} = -\rho\int_{S_0}\left(i\omega_e\varphi(\vec{x}) + \vec{U}\cdot\nabla\varphi_d(\vec{x})\right)n_j ds \tag{2.33}$$

In zero speed condition pulsating Green's function is used . But in this case the body

moves with a certain speed and translating Green's function [16] should be used. The intersection between the free surface and floating body under a forward speed condition makes the boundary integral problem around the hull much more complex than in the zero speed condition and this makes the process of finding the velocity potential is tedious and as well much more time consuming. But in ANSYS AQWA, an alternative approach is used by introducing the speed dependent term to the boundary condition 2.19 which brings the new boundary condition 2.30 this leads to slight change in finding the velocity potential as well. Then the free surface condition specified in the zero speed is used. And then the frequency domain pulsating Green's function can be employed together with the new boundary condition.

RESPONSE AMPLITUDE OPERATOR

The RAO is a transfer function and the essential component in Salvesen method for finding added resistance 2.8. In linear wave theory, RAO is realted to the wave amplitude.

$$\Big(-\omega_e^2 M_{addj} - i\omega_e b_j + C\Big) X_j = F_{jm} \tag{2.34}$$

where F_{jm} is the excitation force, M_{add_j} is added mass and b is damping.

$$X_j = \frac{F_{jm}}{\Big(-\omega_e^2 M_{addj} - i\omega_e b_j + C\Big)} \tag{2.35}$$

However, pulsating Green's function gives similar solution like translating Green's function but in the moderate speed condition where froude number($fn = \frac{U}{\sqrt{gL}}$) should be less than 0.3. Based on this, the speed limit Fn=0.20 & 0.25 are chosen for this research.

3

SOFTWARE COMPARISON

3.1. INTRODUCTION

The program Seaway or Octopus Office and ANSYS AQWA are compared in this section. Seaway was originally written as an algorithm and later merged into the commercial product, Octopus Office. While both Seaway and Ansys AQWA are hydrodymechanic solvers, the solution framework and the options make them different. The computation technique is explained and the comparison between both the software is done in this section. Through this a conclusion is drawn that AQWA will be preferable tool for this research.

3.2. FROUDE SCALING

The standard in marine experiments is to use the Froude method of scaling. Basically, the Froude number (fn) has to be same in model (m) and real scale(R).

$$Fn = \frac{V_m}{\sqrt{L_m g_m}} \tag{3.1}$$

$$\frac{V_m}{\sqrt{g_m L_m}} = \frac{V_R}{\sqrt{g_R L_R}} \tag{3.2}$$

From the above equation, the basic parameters are scaled as:

$$\alpha_T = \alpha_V = \sqrt{\alpha_L}$$

Scaling factor	Scaling
α_L	1:50
α_T	1:7
α_V	1:7

Table 3.1: Scaling factor

In this research, different speeds are mentioned as fn and corresponding values for the model scale are

Fn	Velocity
fn 0.20	1.04 m/s
fn 0.25	1.3 m/s

Table 3.2: Froude number and their speed

3.3. DIMENSION OF ECOLINER

The parameters of the vessel influence on the hydro dynamic co-efficient and the computational time involved in the predicting them. Based on the design proposed by DYKSTRA naval architects the dimension are given in table 3.3. The experiment was done in the towing tank of TU Delft with a scaled model whose ratio is 1:50.

Parameters	Real scale	Model scale
Length	137.9 m	2.75 m
Breadth	18 m	0.36 m
Draft	6.5 m	0.13 m
∇	11600 t	0.092 t
VCG	7.5 m	0.15 m
K_{xx}	5.95 m	0.119 m
K_{yy}	34.35 m	0.687 m
K_{zz}	35.75 m	0.715 m

Table 3.3: Dimension of Ecoliner

The radii of inertia were approximated using the relation

$$K_{xx} \approx 0.30 * B \quad to \quad 0.40 * B \tag{3.3}$$

$$K_{yy} \approx 0.22 * L \quad to \quad 0.28 * L \tag{3.4}$$

$$K_{zz} \approx 0.22 * L \quad to \quad 0.28 * L \tag{3.5}$$

Based on the data described above, the analysis was carried out for the model scale in this thesis.

3.4. COMPARISON BETWEEN SEAWAY AND ANSYS AQWA

Seaway is a computational tool used for finding the ship motions problem in less computational time and it was developed in Delft University of Technology by J.M.J Journee. On the other hand ANSYS AQWA gives a detail analysis of ship motions and the analysis can be performed in both frequency domain and time domain. However in this research for finding added resistance only frequency domain is considered.

ANSYS AQWA

ANSYS AQWA provides a tool set for investigating the effects of environmental loads on floating and fixed offshore and marine structures. The elementary technique used in ANSYS AQWA analysis is Boundary Integration Element method (BIEM). The principle behind BIEM is based on the Green's theorem. ANSYS AQWA uses Hess and Smith constant panel method which is considered to be lower order panel method. ANSYS AQWA can simulate linearized hydrodynamic fluid wave loading on floating or fixed rigid bodies. This is accomplished by employing three-dimensional radiation/diffraction theory and/or Morison's equation in regular waves in the frequency domain. Unidirectional or multiple directional second order drift forces are evaluated by the far-field, or near field solution, or full quadratic transfer function (QTF) matrix. Free floating hydro static and hydrodynamic analyses in the frequency domain can also be performed. Since the analysis is done in frequency domain, Hydrodynamic diffraction feature in ANSYS AQWA is used which mainly focus on the frequency domain and the wave amplitude is considered to be unit amplitude [17].

3.5. RAO COMPARISON

Before getting into RAO comparison, the components that influence the RAO are explained using the figure 3.1. In the low frequency range RAO is influenced by the hydrostatic stiffness and in high frequency range its dominated by mass terms. However the main focus in the sea keeping analysis lies in the intermediate frequencies which are dominated by the

damping terms. These intermediate frequencies are also the most relevant in open seaways where wave-induced resonant motions occur.

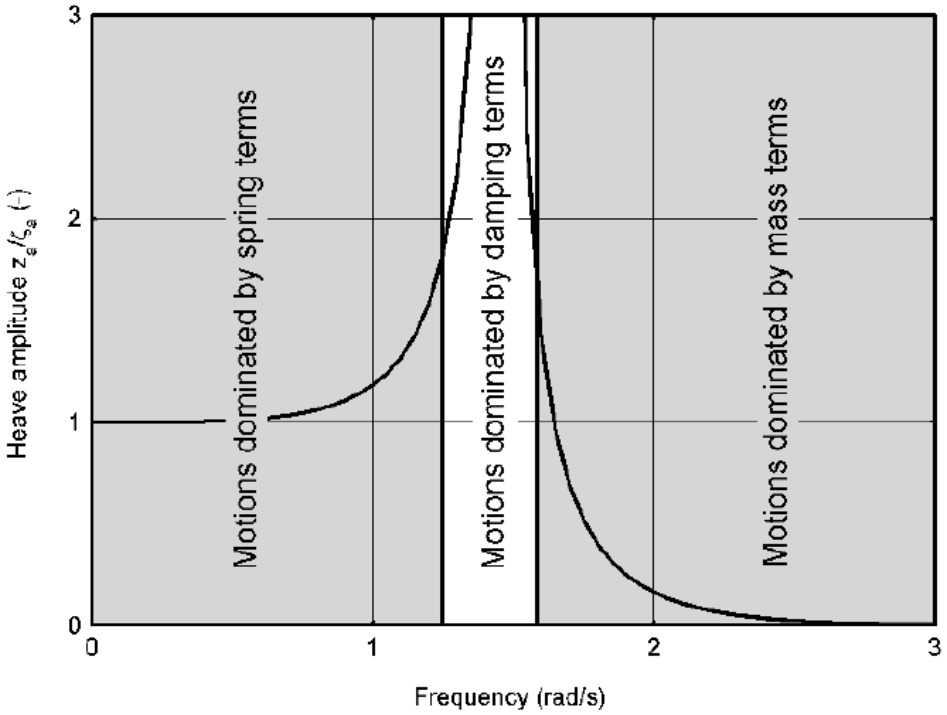

Figure 3.1: Dominant components in RAO

RAO OF UPRIGHT CONDITION FN=0.20

From the figure 3.3 it can be seen that for the low frequency, RAO approaches one. This is because the phase difference between the motion of the ship and the exciting wave is zero. In simple terms, the ship follows the motions of waves in perfect accord. In higher frequency, the response are low because ship length dominate the wavelength so the ship does not react to the wave and as a result RAO approach to zero in high frequency. As the speed increases, the peak of RAO also increases, this is due to speed dependent term i.e. encounter frequency. This is relevant to the heave and pitch motion RAOs considered here.

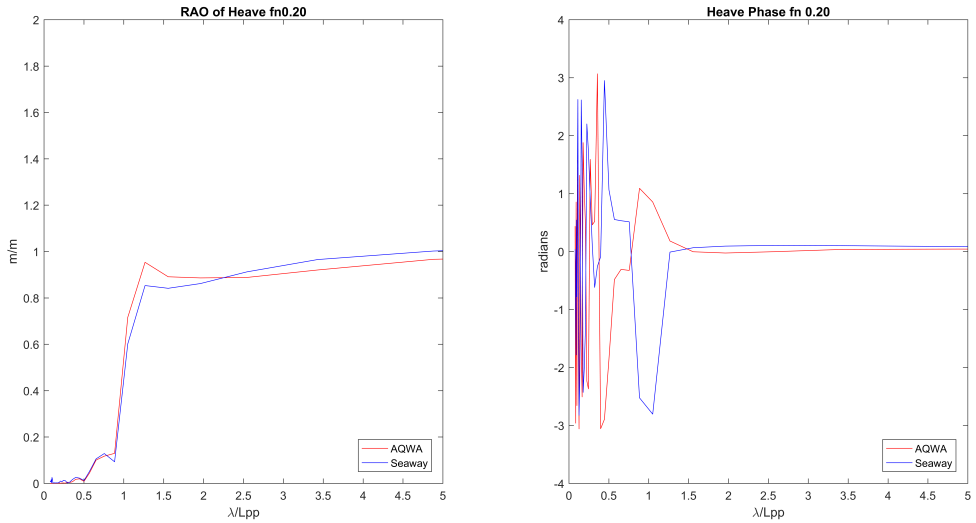

Figure 3.2: Heave RAO comparison upright condition fn=0.20

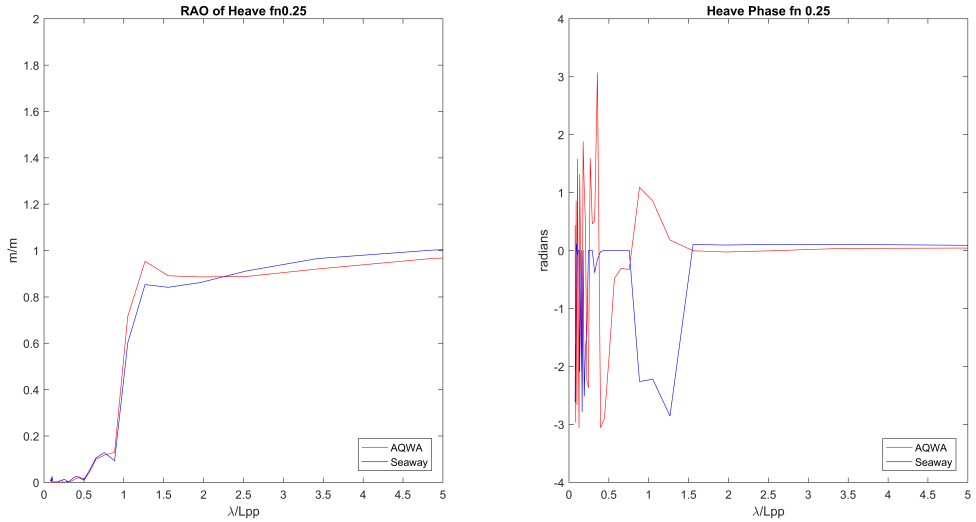

Figure 3.3: Heave RAO comparison upright condition fn=0.25

In the heave RAO fig 3.3, the high frequency coincides well as the wave approaches the long waves the difference in the Seaway and ANSYS AQWA could be seen. In phase figure, the intermediate frequency are outphase and very long waves the both tool are in phase.

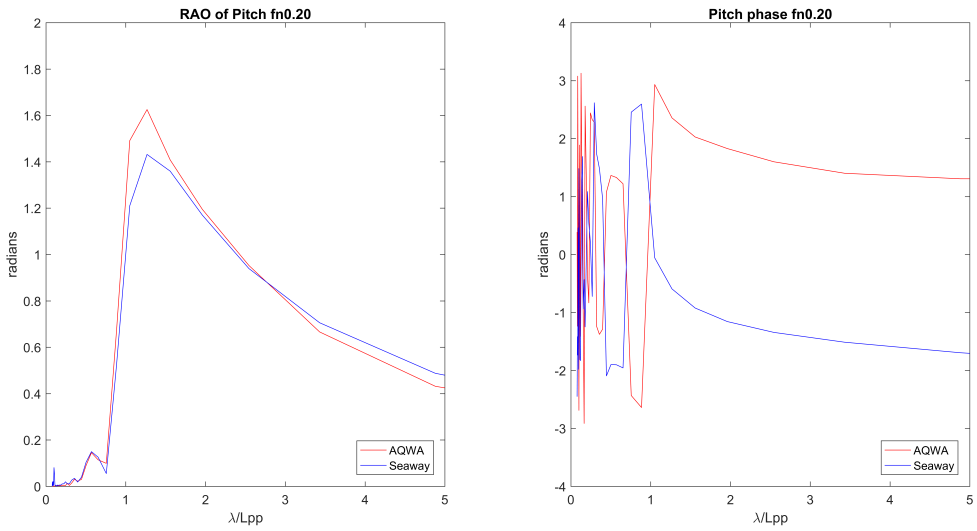

Figure 3.4: Pitch RAO comparison upright condition fn=0.20

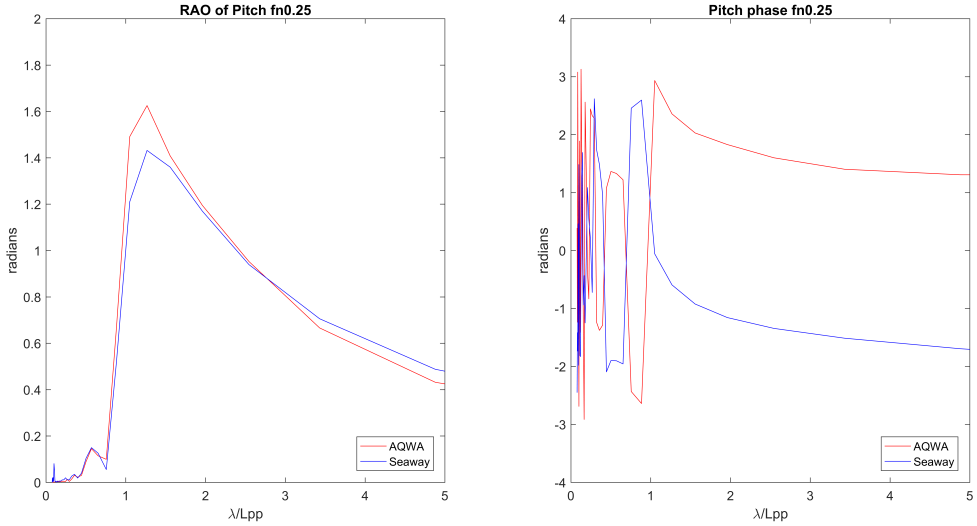

Figure 3.5: Pitch RAO comparison upright condition fn=0.25

In pitch RAO, there is the difference in peak value of pitch in the both speeds and there is phase shift between the Seaway and ANSYS AQWA results.

3.6. WAVE FORCE COMPARISON

TOTAL WAVE EXCITATION FORCE COMPARISON

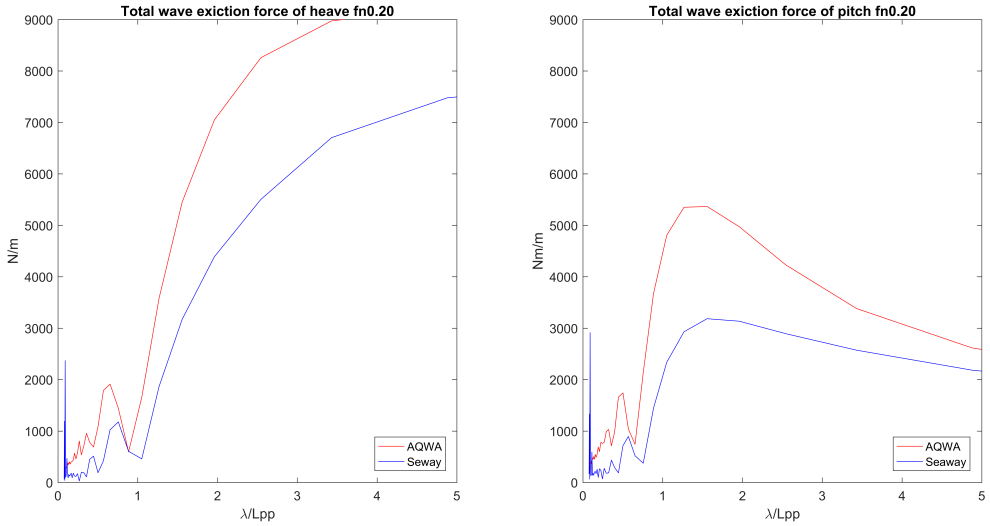

Figure 3.6: Total wave excitation force upright condition fn=0.20

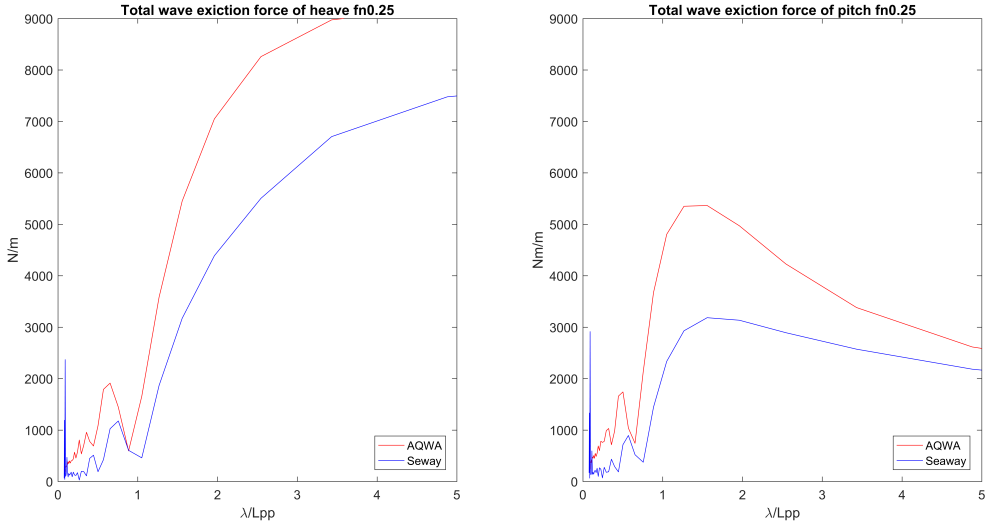

Figure 3.7: Total wave excitation force upright condition fn=0.25

$$F_{tot} = F_{fk} + F_d + F_r \tag{3.6}$$

The first two terms on the right side of the equation 3.6 are wave excitation force. The way Froude Krilov force is determined is similar in both the software packages but not for the diffraction force. As you could see the difference in the values in both heave and pitch are high for low frequency range and results were satisfactory in high frequency. I believe, the strip theory does not works well for low frequency because the free surface boundary condition do not satisfy in the low frequency [18]. And this could be reason difference in

the values of heave and pitch.

In octopus office Haskind assumption is followed which states that the diffraction force is equal to radiation force. In Aqwa diffraction potential is determined from the translating Green's function [16] and then diffraction force is calculated. This difference in the computation technique might have played a role.

3.7. CONCLUSION

Generally, ANSYS AQWA is used for zero forward speed. In order to justify computational method of ANSYS AQWA with forward speed, a comparison is done with Octopus Office which was developed in TU-Delft was used. However both the methods uses different approach, one is boundary element method and other strip theory respectively. The difference in the results between two programs has high discrepancy. However ANSYS AQWA takes higher computational time than the octopus office. Despite the drawback, ANSYS AQWA is capable of performing computation even in asymmetric water plane which is the main goal of thesis.

4

NUMERICAL ANALYSIS

In this section a detailed description of the results from numerical analysis for this thesis is given. The first part of the chapter explains about added resistance and factors influencing it. In latter part, the required parameters for analysis is found using ANSYS AQWA and a description follows how added resistance is determined numerically.

PARAMETERS FROM ANSYS AQWA

The main parameters required to describe the Salvesen method as per in the equation 2.5 are Froude Krilov force, diffraction force, RAO, their phases and the values are predicted from ANSYS AQWA and the results are given below

4.1. RAO

The added resistance is influenced by the relative vertical motion as stated in the section 2.8 and it can be determined from the motions of the heave and pitch. The RAO obtained from ANSYS AQWA are coupled RAO, which state that if there is an extreme motion in one degree of freedom and this will affect the motion on the other degree of freedom as well. The values were made non-dimensional [9] by dividing them with the unit wave amplitude

.

4.1.1. HEEL CONDITION

HEEL HEAVE RAO

The RAO of heave for the upright and heel 10 condition has the similar trajectory but in heel 20 at , there is a sudden rise around the value of $\lambda/L_{pp} = 3.25$. I believe this shift occurs due to the combination of two reasons, the encounter frequency experienced by the model

matches with the natural frequency of the roll motion which causes resonance and added to that the distribution of pressure is strong on one side (starboard) and weak on other side (port side) under heel 20. This pressure difference generates an uneven force distribution and this eventually leads to instability of the vessel and this effect could be seen in the figure 4.1. The responses are in phase for the upright and heel 10 conditions but there is a slight deviation in the heel 20.

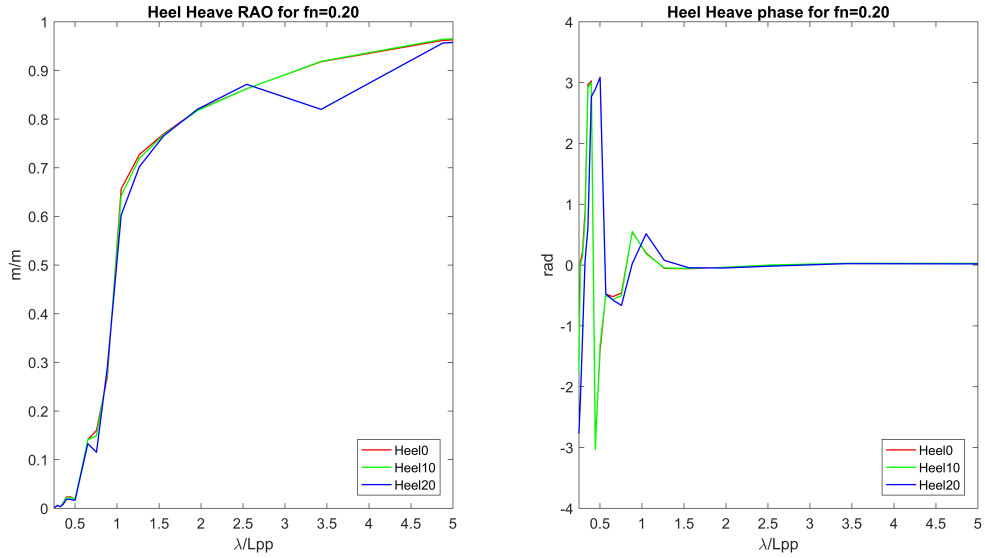

Figure 4.1: Heave RAO for Heel condition fn=0.20 and its phase

As calculated below, this is seen to be the natural frequency for the roll response. The current software setup in AQWA cannot give a reliable physical amplitude at this resonant condition. Therefore at this point no conclusions regarding the motion amplitude can drawn.

$$\omega_n = \sqrt{\frac{c_{\phi\phi}}{I_{xx} + A\phi\phi}} \tag{4.1}$$

$$c_{\phi\phi} = \rho g \nabla \cdot GM \tag{4.2}$$

By solving the above expression with our known values, the natural frequency found to be $\lambda/L = 3.2$ ($2.88 rad/s$) which is around the encounter frequency experienced by the model in heel 20 at fn=0.20.

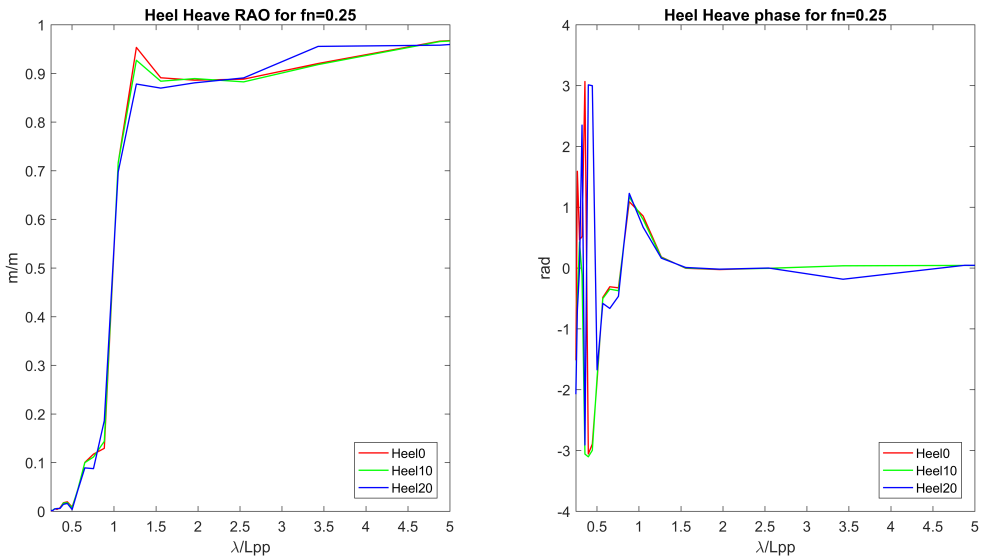

Figure 4.2: Heave RAO for Heel condition fn=0.25 and its phase

HEEL PITCH RAO

The influence of roll motions is slightly seen in the figure 4.3 but not that high as heave and roll coupling [19] (figure 4.1). However there is a phase lag between upright and heel 20 in the intermediate frequency range and the phase decreases at $\lambda/L = 3.2$. But in the case of fn=0.25, the pitch RAO (figure 4.4) is not affected by extreme roll motion because encounter frequency does not match the the natural frequency of roll but the influence can be seen in the both phase figure 4.3 & 4.4

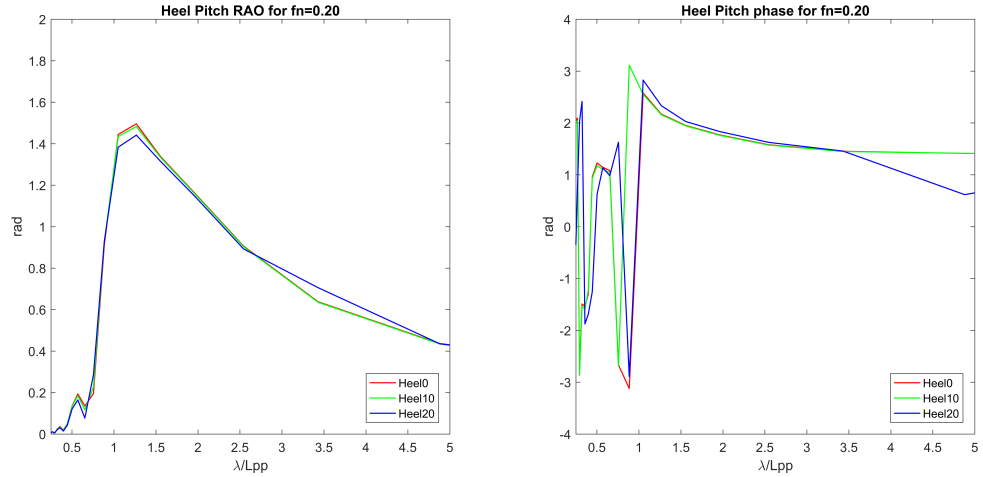

Figure 4.3: Pitch RAO for Heel conditions fn=0.20 and its phase

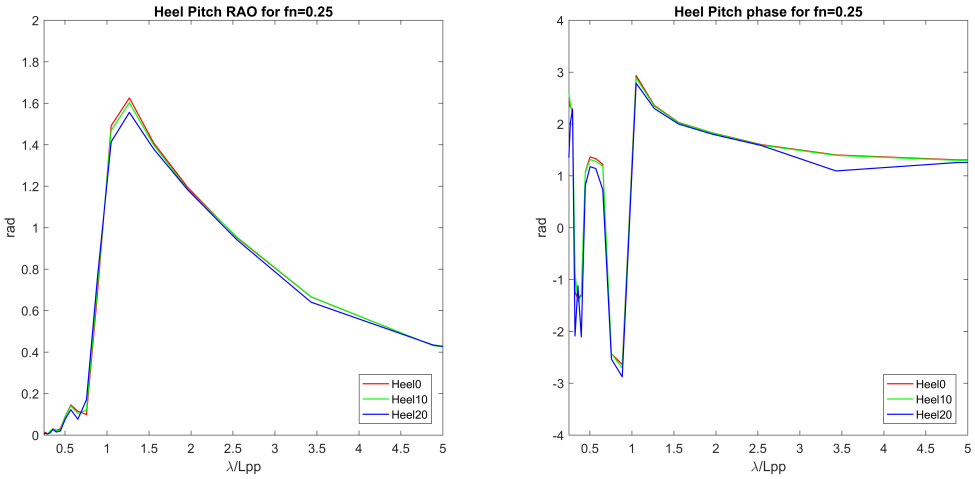

Figure 4.4: Pitch RAO for Heel conditions fn=0.25 and its phase

4.1.2. LEEWAY CONDITION

LEEWAY HEAVE RAO

The discrepancy between the RAO values in the figure 4.5 are explained as follows. Initially, the correlation between the values can be seen in the high frequency range and in this range wave excitation force is considered to be low low. Despite this, it experience the reflection components they seems to be similar in both leeway and upright conditions. As the graph moves further from the high frequencies, the discrepancy between the RAO values increases because of the change in wetted surface area.

The phase slightly coincides with each other but in when wavelength is equal to one there is change in the phase between upright and leeway conditions. In low frequency range, the values start to converge because the ship motions are in phase with the wave so there will not be significant radiation or reflection components.

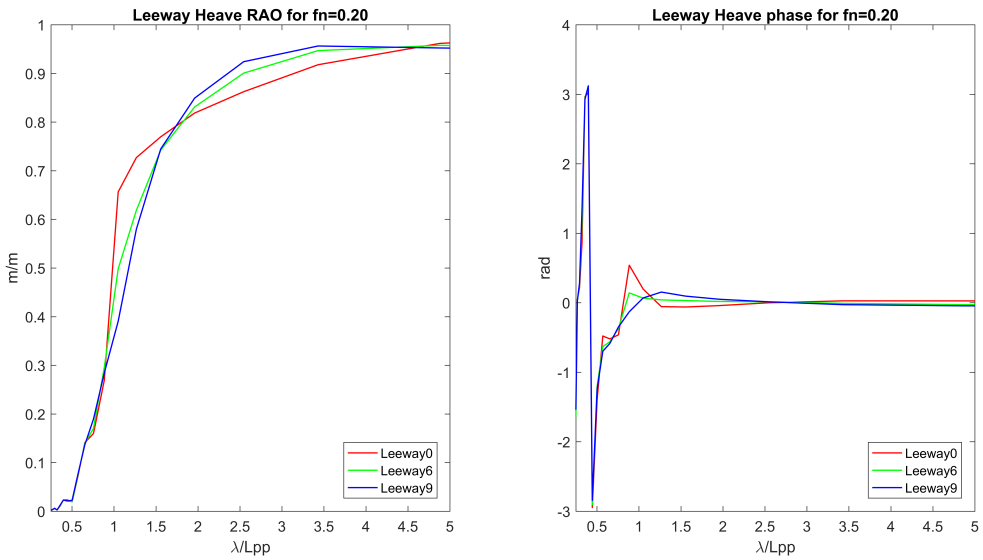

Figure 4.5: Heave RAO for Leeway condition fn=0.20 and its phase

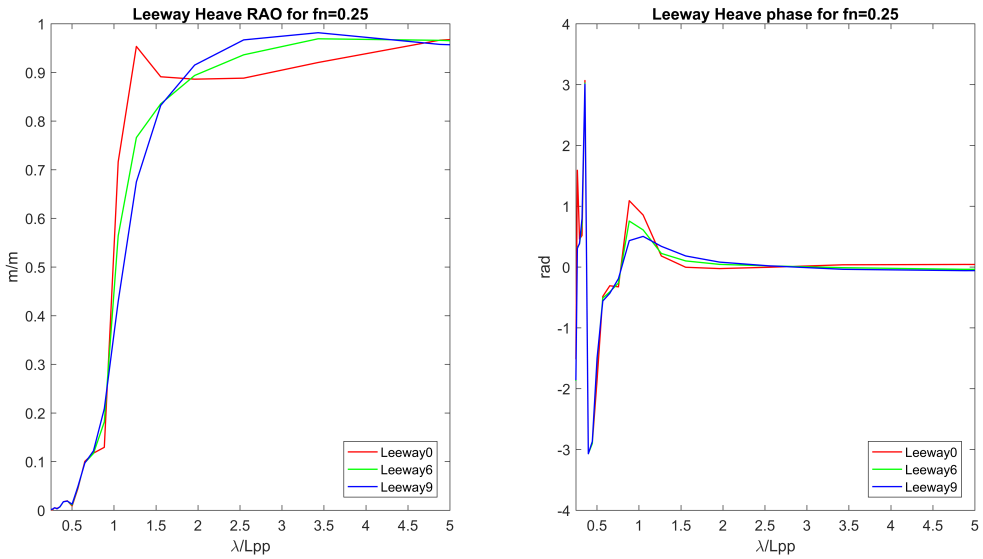

Figure 4.6: Heave RAO for Leeway condition fn=0.25 and its phase

LEEWAY PITCH RAO

From the figure 4.7 & 4.8 the difference in pitch RAO is high compared to heave RAO under leeway condition. Because of the position of the model in the leeway condition the wave hits around the blige region 4.1.2. This in turn generates hydrodynamic pressure high on the one side of the model and lower on the other side of the model (leeward region) and this high asymmetric pressure distribution on the hull which is not seen in the case of upright . On the other hand the coordinate system followed for leeway conditions is not same as in the upright condition. In leeway conditions (especially for the 9 degrees), the pitch response is slightly affected by the presence of roll.

This axis definition influence in the phase figure 4.7 & 4.8 also, as it can be seen there is a phase shift as the leeway increases.

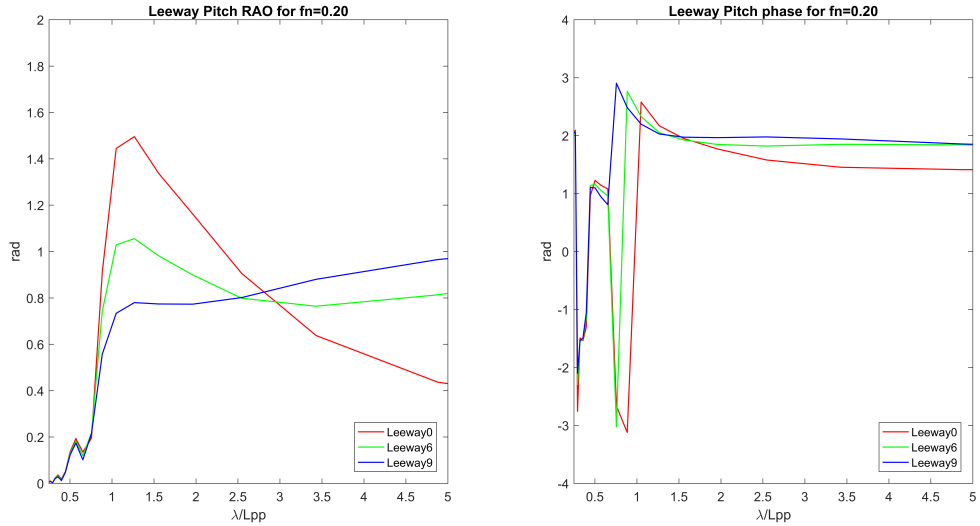

Figure 4.7: Pitch RAO for Leeway conditions fn=0.20 and its phase

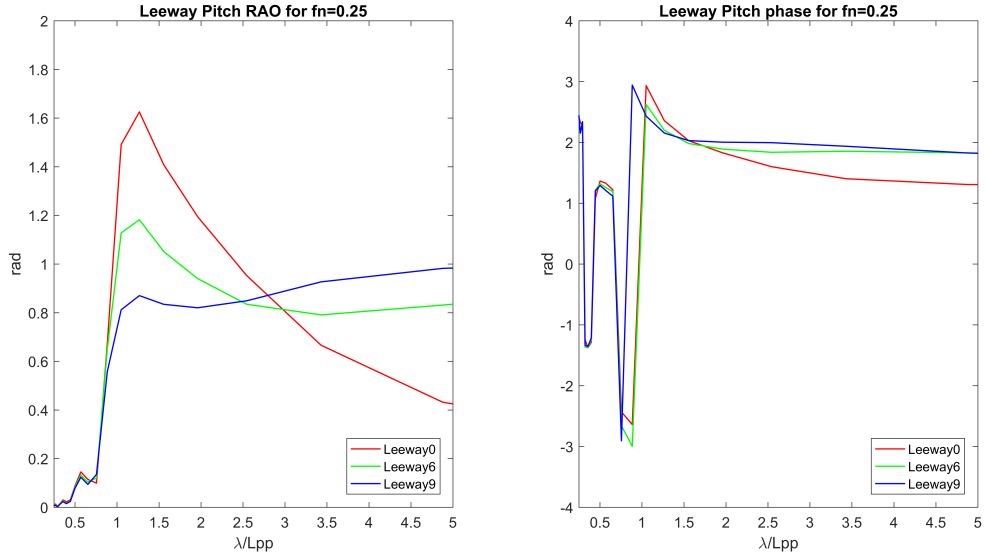

Figure 4.8: Pitch RAO for Leeway conditions fn=0.25 and its phase

4.2. WAVE EXCITATION FORCES

4.2.1. FROUDE KRILOV FORCE

The Froude Krilov force is a wave force due to undisturbed wave acting on a body. The main input for finding this force is the wetted surface of the hull and this shows the there is no influence due to forward speed. The same principle is applicable for the pitch conditions as well

Note: For the sake of simplicity, the basic six degrees of freedom force solution in AQWA has been used without post-processing for these results.

Which implies that the freedom given to roll motion (unlike in the experiment) may play a minor role in the Froude-Krylov results seen for heave and pitch.

This difference is acknowledged and it is not considered important since describing the incoming waves is not the focus of this work. However, experimentally constrained roll is a valid feature and included in the added resistance plots, which are the main focus of this study.

4.2.2. HEEL CONDITION

HEAVE

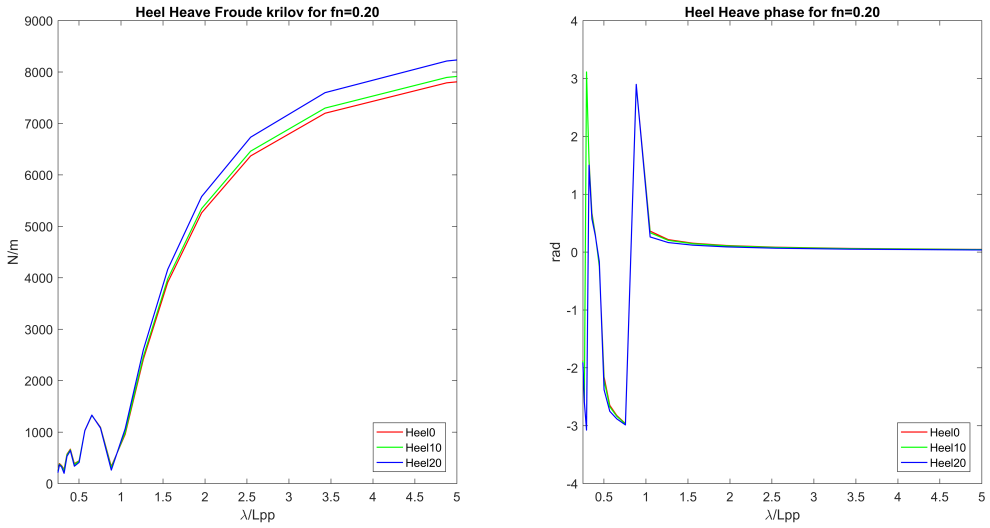

Figure 4.9: Heave Froude Krilov for Heel condition fn=0.20 and its phase

PITCH

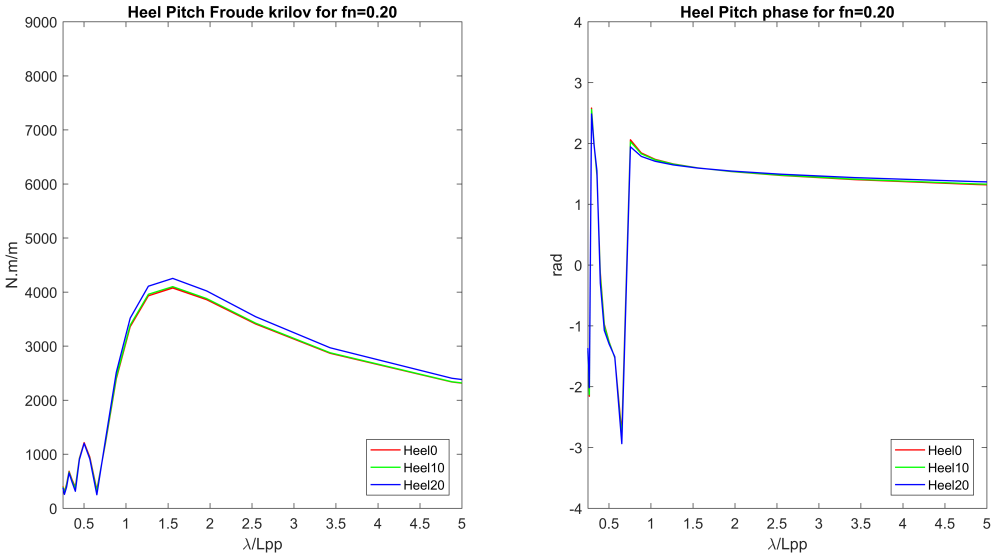

Figure 4.10: Pitch Froude Krilov for Heel condition fn=0.20 and its phase

4.2.3. LEEWAY CONDITION

HEAVE

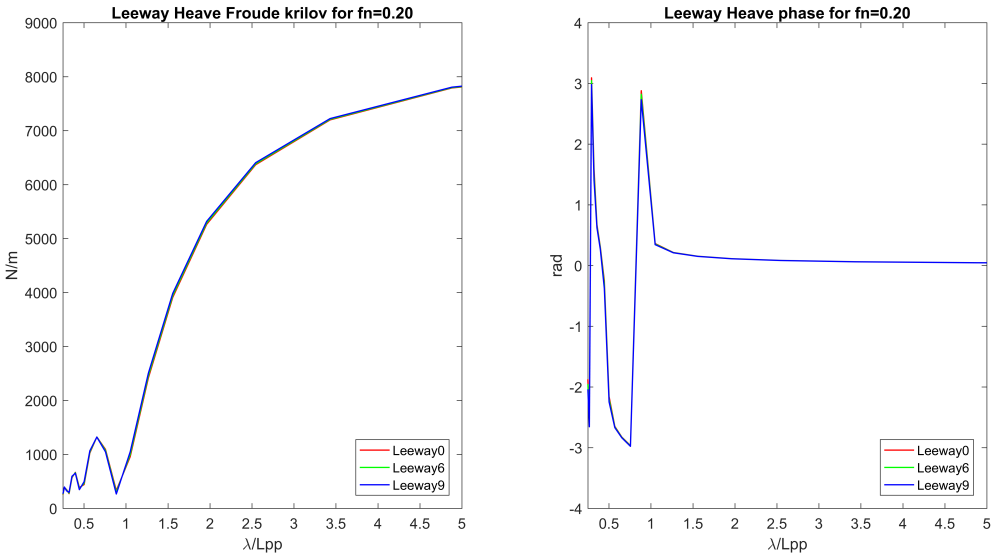

Figure 4.11: Heave Froude Krilov for Leeway condition fn=0.20 and its phase

PITCH

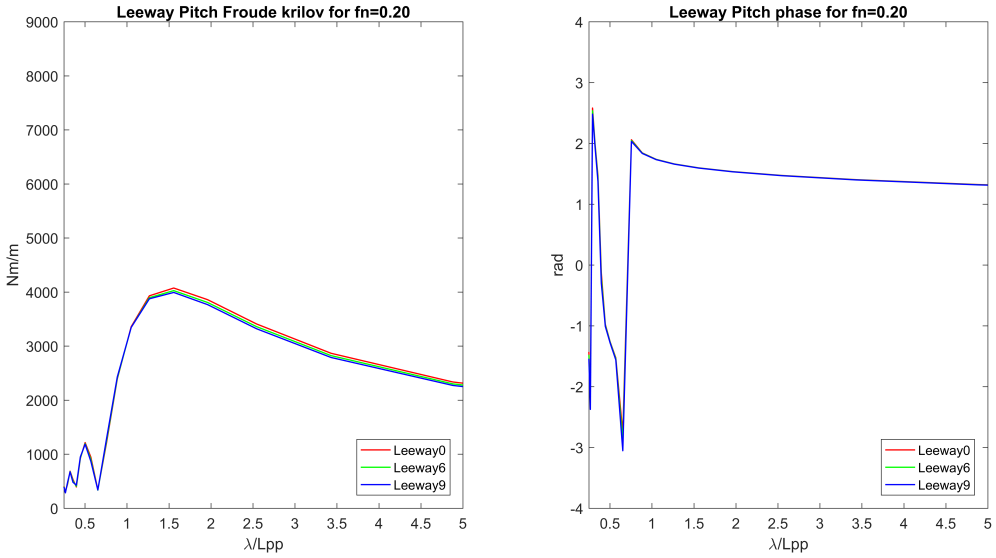

Figure 4.12: Pitch Froude Krilov for Heel condition fn=0.20 and its phase

From the figure Heel Froude Krilov force 4.9 & Leeway Froude Krilov 4.11, a trend can be seen that in high frequencies the froude krilov values are similar for different heel conditions where as in the low frequency, the froude krilov increases as the wetted hull surface area increases. And in case of phase three conditions coincides well with each other and there is slight increase around $\lambda/Lpp = 1.25$. The similar trend is followed in pitch 4.10 & 4.12

4.2.4. DIFFRACTION FORCE

In the context of the scope of this thesis, diffraction purely means the scattered/ reflected wave component off the body. This component in addition to the Froude-Krylov wave form the total diffraction load component.

Note: As noted previously, the basic six degrees of freedom force solution in AQWA has been used without post-processing for these diffraction force results as well.

4.2.5. HEEL CONDITIONS

HEAVE

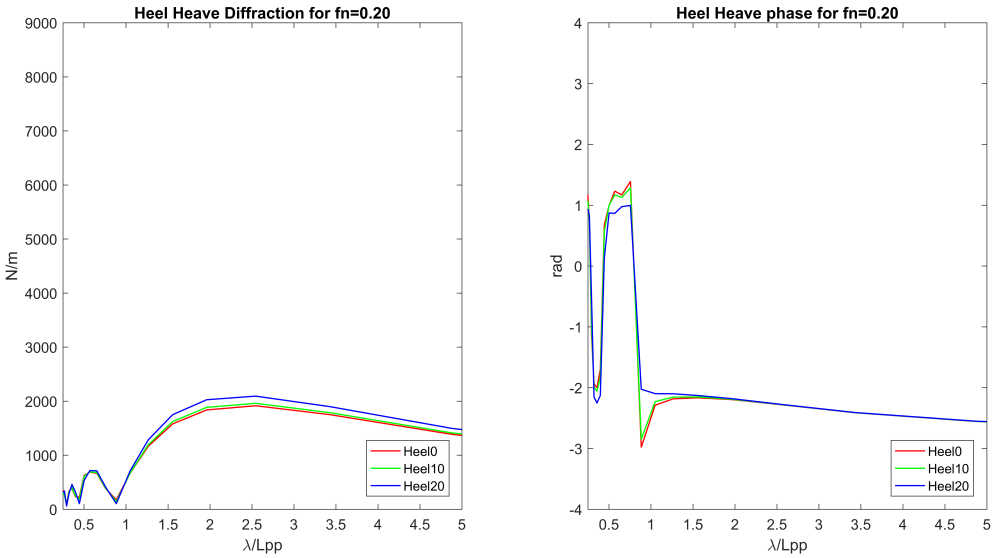

Figure 4.13: Heave Diffraction force for Heel condition fn=0.20 and its phase

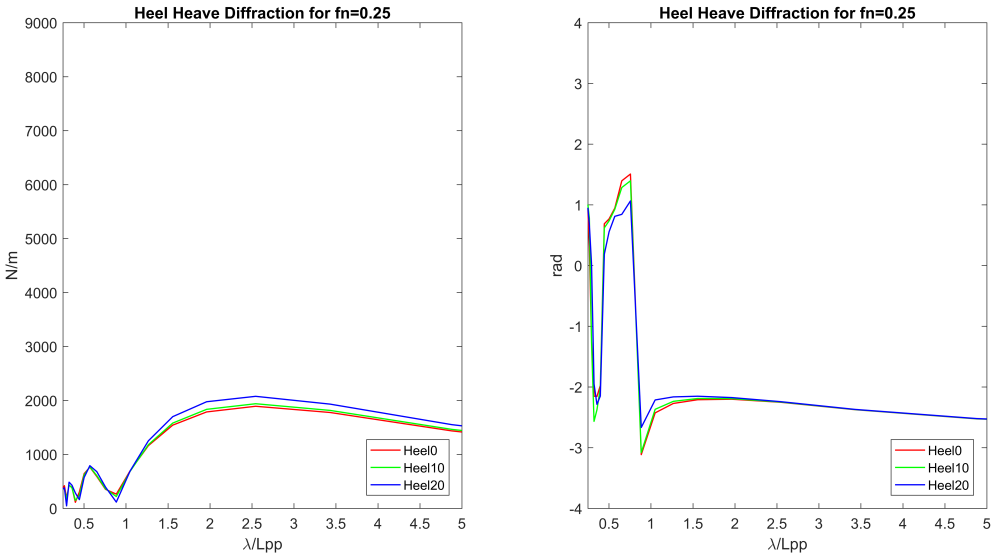

Figure 4.14: Heave Diffraction force for Heel condition fn=0.25 and its phase

From the figure 4.13 & 4.14, it can be seen as the wetted surface area increases the diffraction forces as well increases with respect to different frequencies. Unlike Froude Krilov force there is slight variation in phase plot around the intermediate region. This description can be applied to pitch mode as well.

PITCH

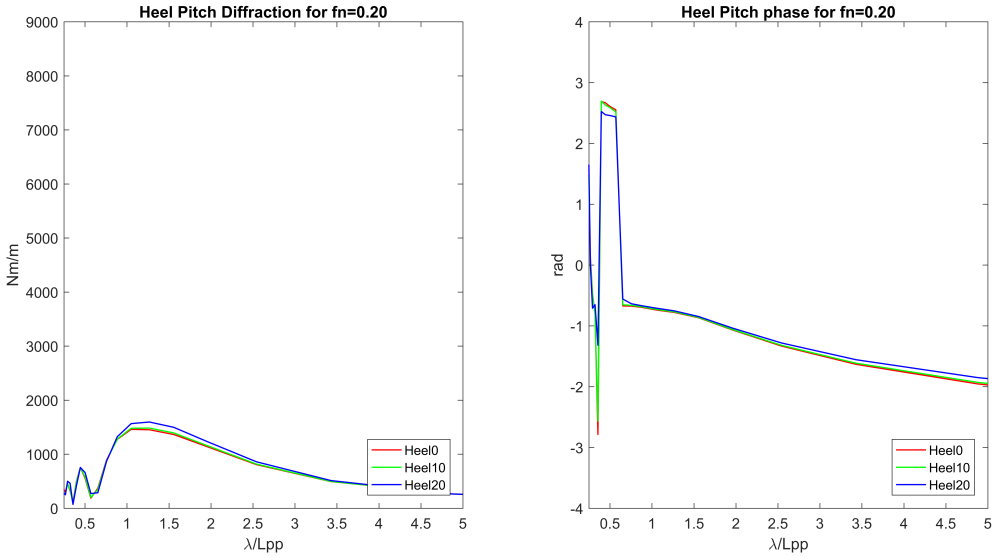

Figure 4.15: Pitch Diffraction moment for Heel condition fn=0.20 and its phase

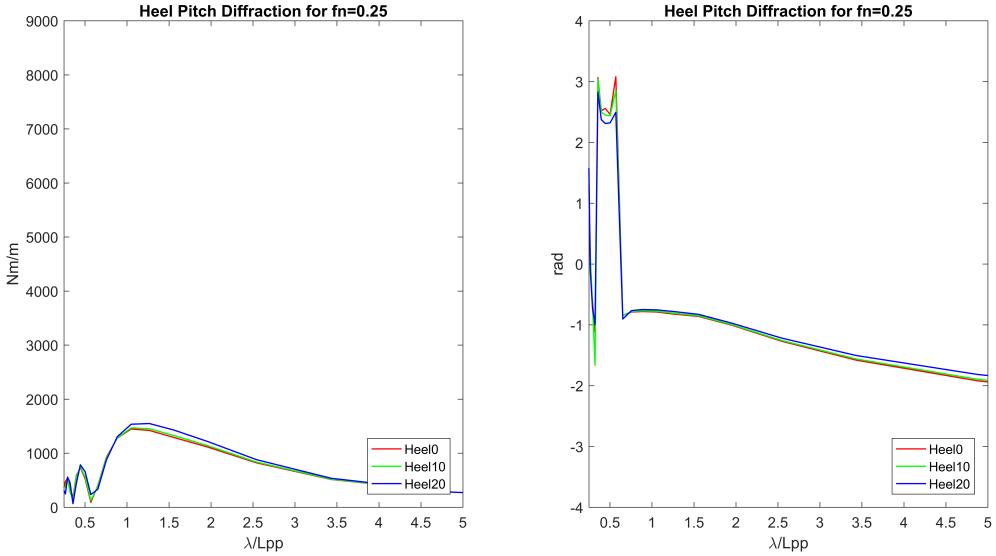

Figure 4.16: Pitch Diffraction force for Heel condition fn=0.25 and its phase

4.2.6. LEEWAY CONDITIONS

HEAVE

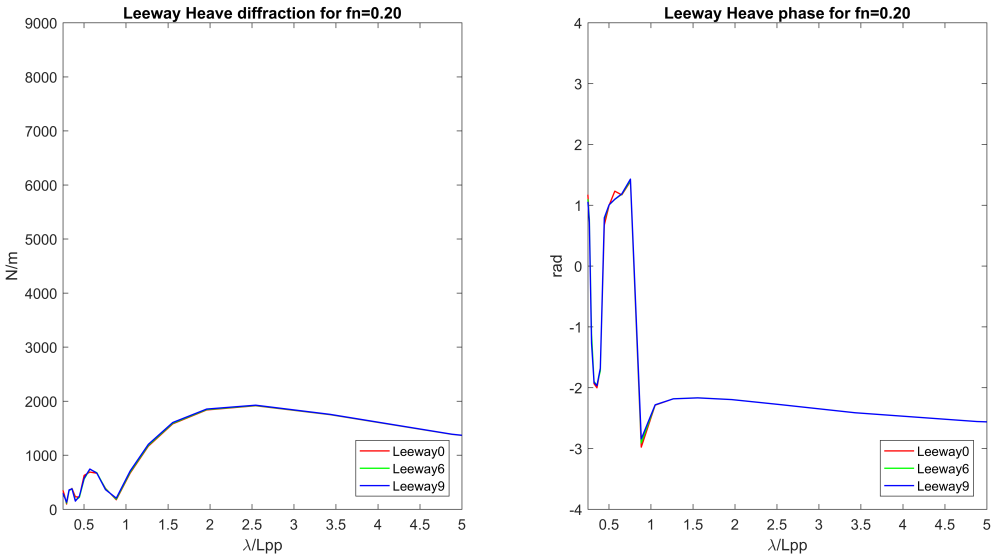

Figure 4.17: Heave Diffraction force for Leeway condition fn=0.20 and its phase

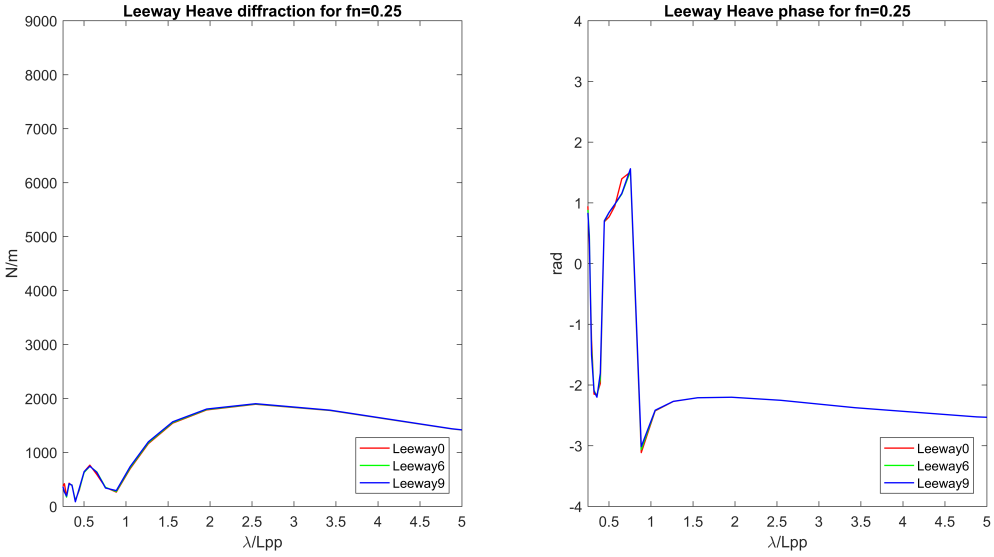

Figure 4.18: Heave Diffraction force for Leeway condition fn=0.25 and its phase

The figure 4.17 & 4.18 shows the diffraction force in leeway condition for heave, shares the same trajectory and the values are approximately equal as well and in the case of the phase follows same trend and the values matches well for the entire frequency range. It is pointed out again that the correlation is without the effects of a constrained roll.

PITCH

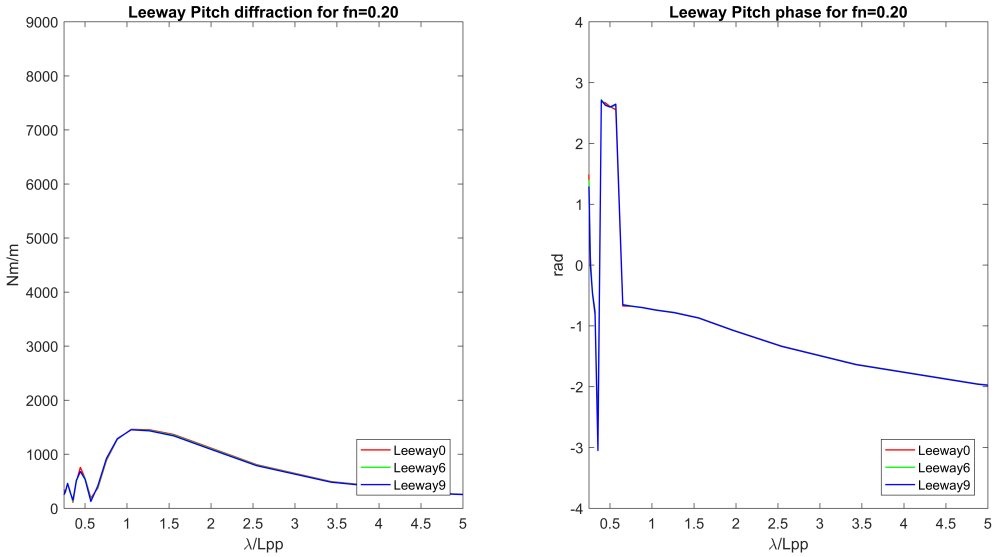

Figure 4.19: Pitch Diffraction moment for Leeway condition fn=0.20 and its phase

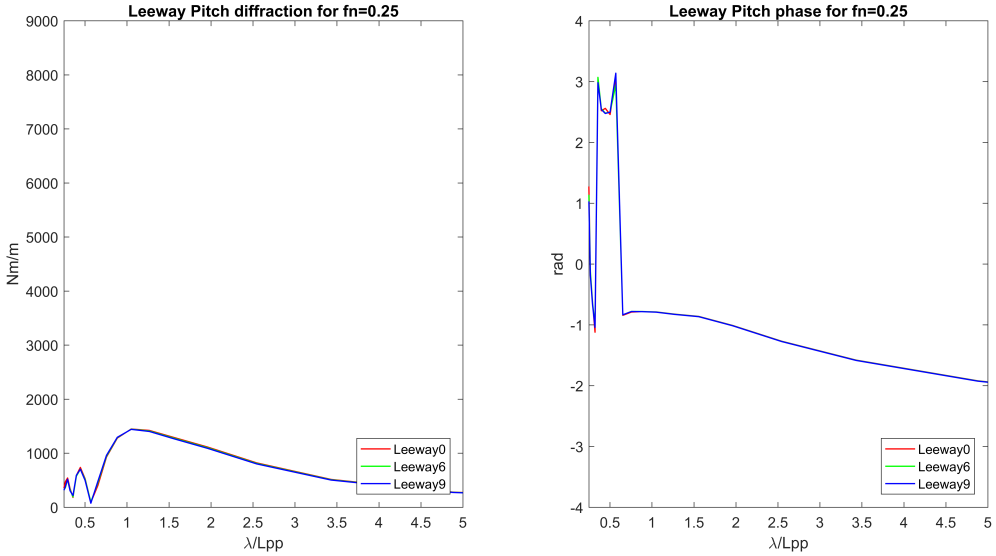

Figure 4.20: Pitch Diffraction force for Leeway condition fn=0.25 and its phase

4.3. ADDED RESISTANCE PREDICTION

The essential parameters are obtained from above section and the added resistance is predicted using Salvesen method. The predicted values of added resistance are made dimensionless using the empirical relation 4.3

$$R_{aw_{nd}} = \frac{R_{aw}}{(\rho g \zeta_a^2 B^2 / L)} \tag{4.3}$$

In the above equation, as said in the section 4.1 wave amplitude is taken to be unity and length and breadth values are taken in model scale.

HEEL ADDED RESISTANCE

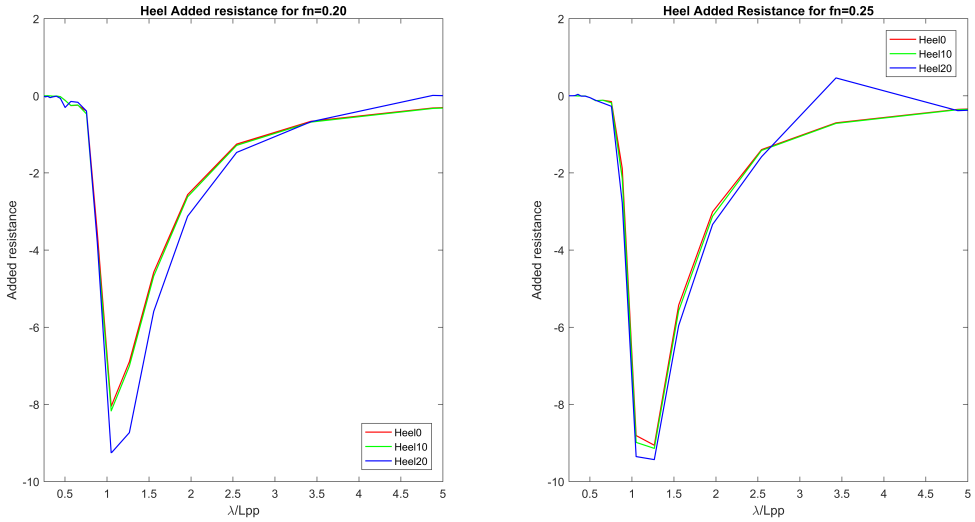

Figure 4.21: Added resistance for Heel condition

Left-side of the figure 4.21 shows, for the higher frequencies the added resistance is almost approaching zero. This is because as stated in the section 2.8, the relative vertical motion is negligible at this frequency range because of the absence of motion induced component. In very low frequency the added resistance also approaches to zero this is because the ship and waves are in phase.

However, the highest magnitude of added resistance is found when the wave length is equal to the ship length. As the heel angle increases the added resistance increases relative to the upright condition. But, in heel 20 at the speed of fn=0.25 and when $\lambda/L_{pp} = 3.25$ a sudden rise was found in the figure for heave 4.2 which was explained in the section 4.1.1.But, from the figure 4.1 it can be seen that the decrease in Heave RAO is countered by the increased pitch RAO compare to other conditions and this in turn maintains the added resistance.
In the figure 4.21, it is seen that the added resistance increases with the speed (fn=0.25) and still the maximum value of added resistance holds in $\lambda/Lpp = 1.25$. In other words, the ship length: wave length ratio of about 1 is still the point of maximum resistance but it seems to occur at a slightly higher wavelength (period) because of the increased forward speed effect.

4.4. DIFFERENCE IN PRESSURE DISTRIBUTION

Before explaining the results of added resistance in leeway conditions. I would like to explain the variations in the pressure distribution between upright and leeway conditions with the help of figure 4.22 & 4.23. In order to compare the difference, the ratio '$(\lambda/L \approx 1)$' is taken because at this frequency maximum value of added resistance is found.

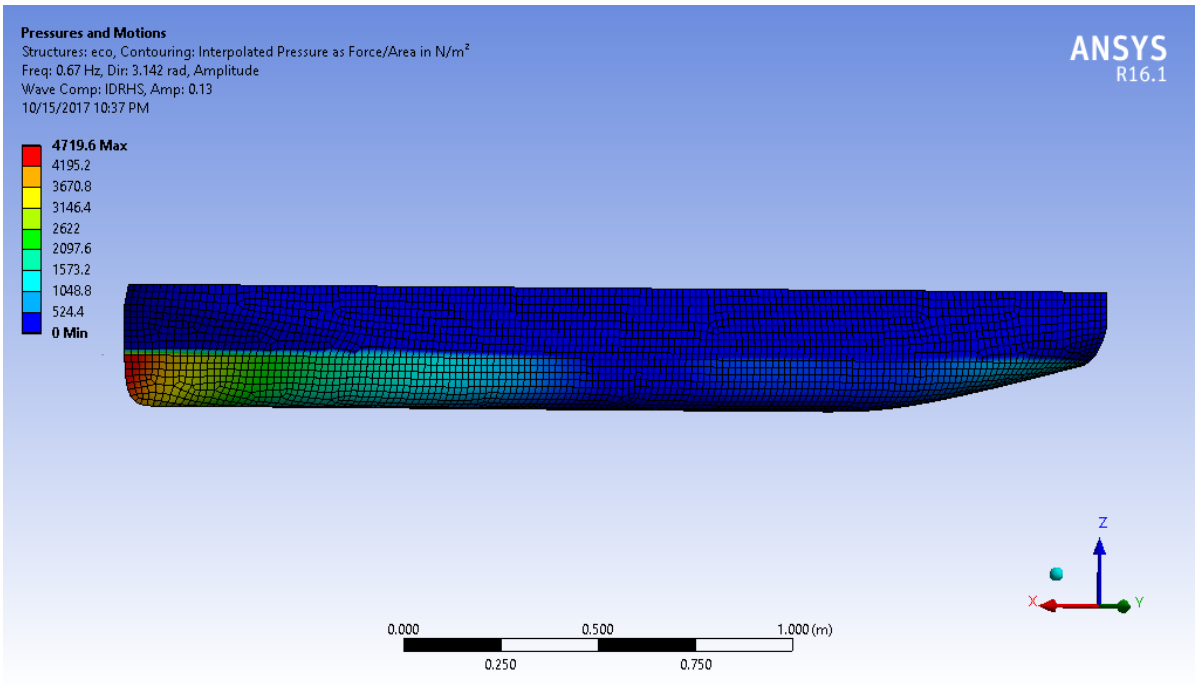

Figure 4.22: Pressure distribution in upright conditions

It can be seen that, the pressure distribution contour looks similar in the both cases but the amplitude differs.

In upright condition the peak value is around 4600 N/m^2 and the maximum global pressure is much lower at around 1500 $N/m^2$and often less.

In upright condition, the port side and starboard side are completely symmetrical in terms of pressure distribution. The port side is shown in the figure 4.22.

For the leeway case with 9 deg heading there is a distinct difference between the windward and leeward side. The leeward half ie. the port side is shown here and true to expectation the pressure is lower than for the upright case.

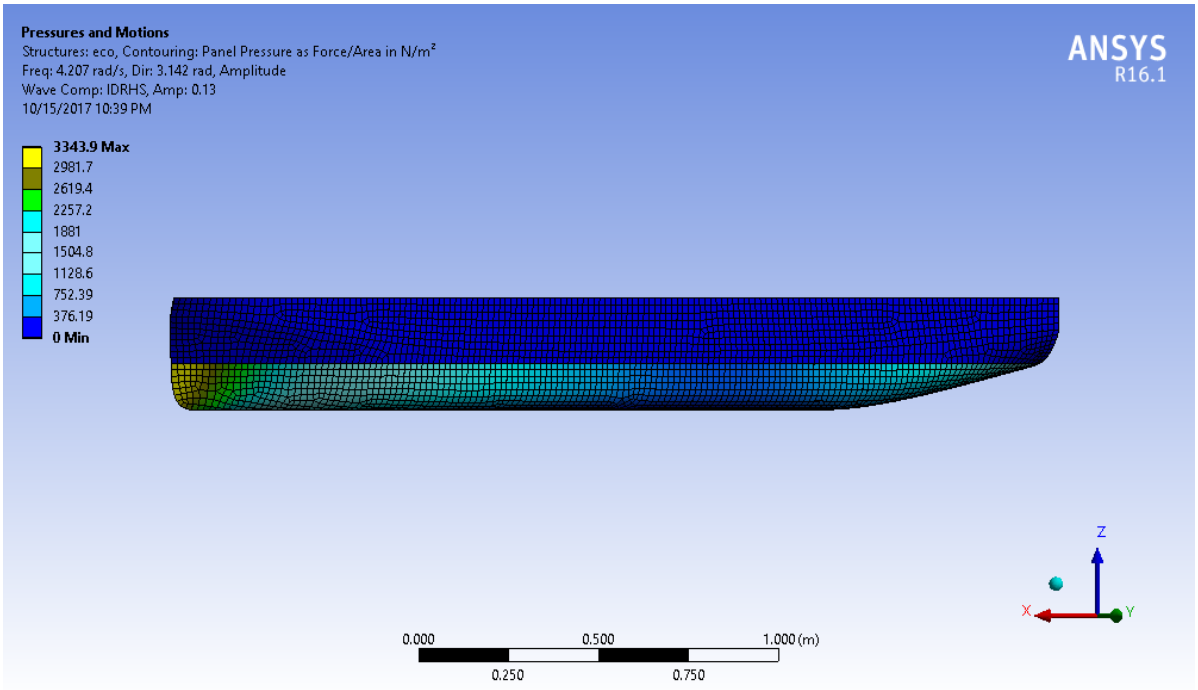

Figure 4.23: Added resistance for Leeway condition

where as in the leeway conditions, the peak value is around 3000 N/m^2 but the the global pressure distribution in the hull is about 300 N/m^2. As said in the section 3.4, computation in ANSYS AQWA is done with the the help of pressure in each panel. Since the pressure in the leeway condtion is relatively lower than in the upright conditions and I believe this could be the reason for the much difference between upright and leeway conditions.

LEEWAY ADDED RESISTANCE

From the left figure 4.24, the difference between the upright condition and leeway which is high even though water plane area is more over similar to each other. In upright condition or heel condition the bow faces the head faces where as in leeway the point of contact between the wave and model will be on the rounded bilge part towards starboard. The difference between these two scenario were explained in section 4.1.2

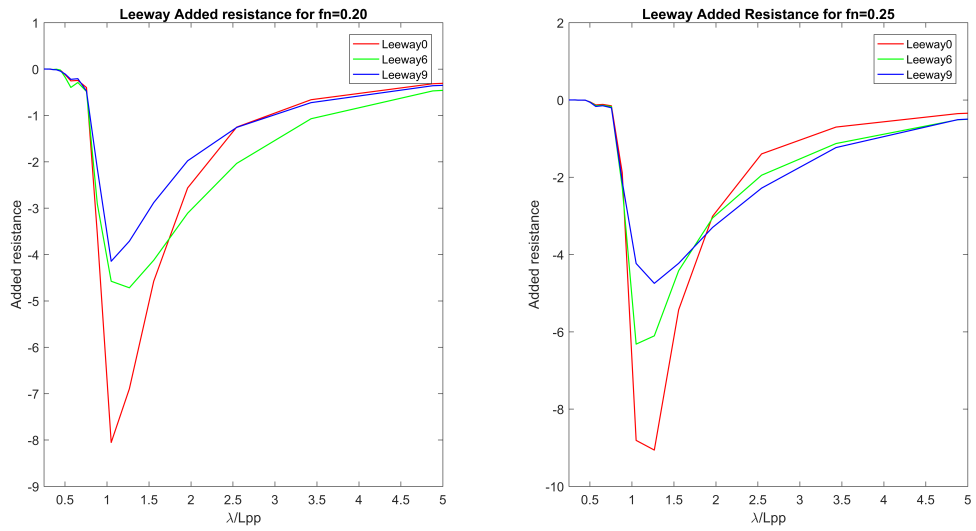

Figure 4.24: Added resistance for Leeway condition

The added resistance increases with the forward speed as shown in right figure 4.24 but the occurrence of maximum value didn't change in both forward speed. Unlike heel condition the trajectory is similar in for both forward speeds.

4.5. ROLL INFLUENCE IN LEEWWAY

As stated in the section 4.1.2, the dominance of the roll can be clearly seen in the following figure 4.25 & 4.26. The axis definition for upright and leeway are shown in the fig 4.27, in leeway 6 the 'y axis' inclined w.r.t the center line of the model and the rotation along this axis is not purely pitch but it has the influence of roll as well.

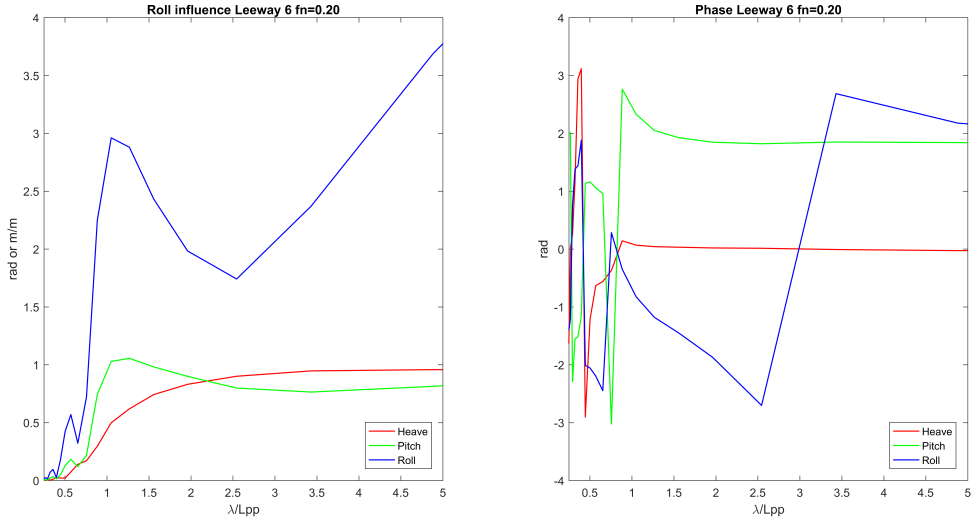

Figure 4.25: Roll dominance in Leeway 6 condition fn=0.20 and its phases

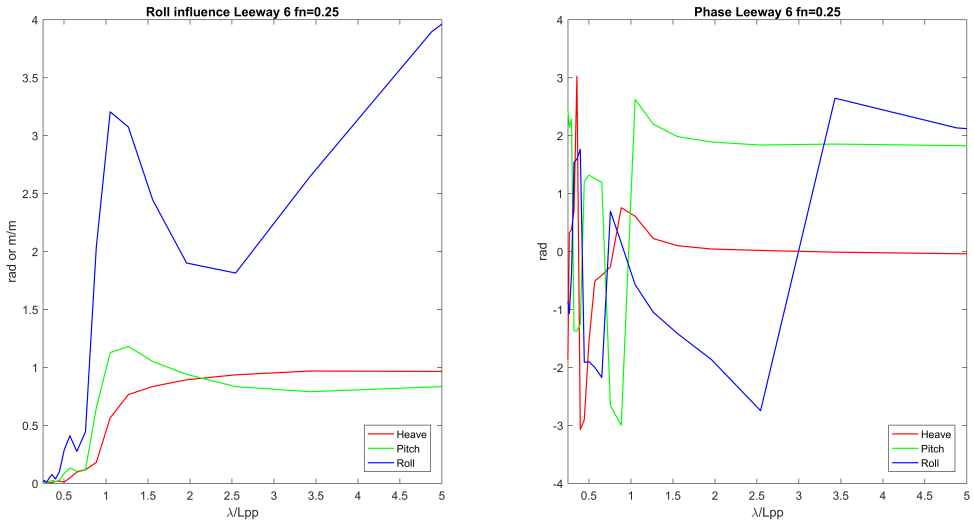

Figure 4.26: Roll dominance in Leeway 6 condition fn=0.25 and its phases

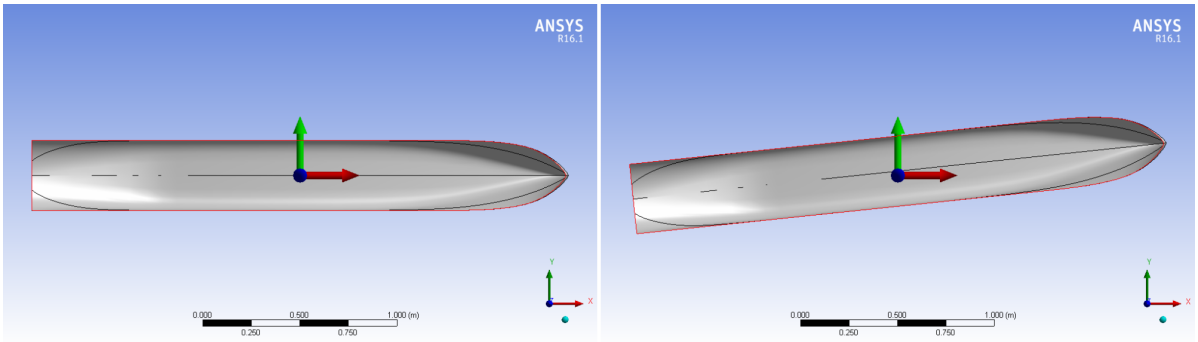

Figure 4.27: Axis definition in Upright and Leeway 6 condition

In order to check this issue, point is chosen with the co-ordinates (1,1,1) w.r.t the model and the relative motion of this particular point is studied using the relation 4.4.

$$z_p(t) = z(t) - x_{bp}\theta + y_{bp}\phi(t) \tag{4.4}$$

From the figure 4.28 it can be seen that, relative vertical motion of the point follows the similar trend of roll and this clearly shows the roll influence in the resulting vertical motion. By extension it can also be seen that constraining such a roll motion contributes to the added resistance which is the most important parameter of the research thesis.

The analyses done so far were properly used to appreciate the effect of constraining the roll motion, as the experiment was carried out. For the added resistance plots, the same six DOF solution in AQWA is the basis. However, to describe the force component that a constrained roll restricted for the experiment, some post-processing has done.

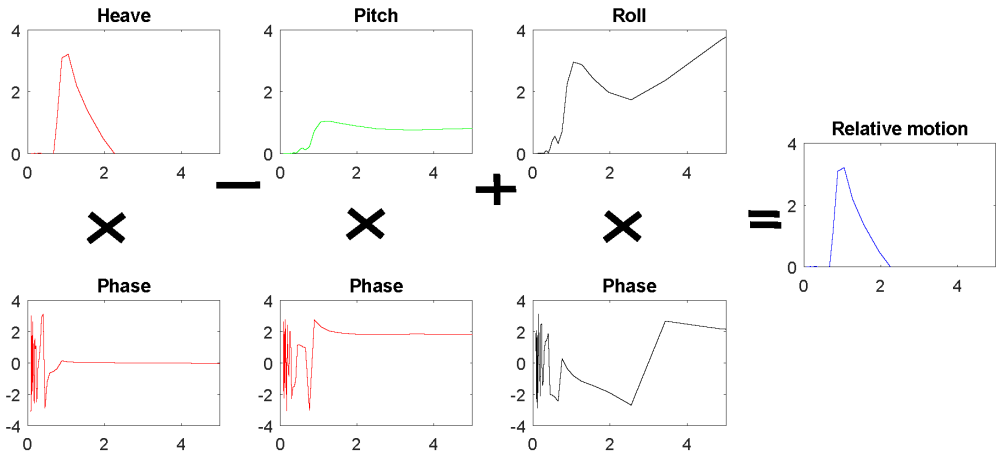

Figure 4.28: Relative vertical motion

The roll load RAOs were extracted from the numerical results and fed back to the added resistance term with the proper amplitude and phase information. In the experiment that was performed only the heave and pitch motions were allowed. In particular, the constraint of roll (and to a much lesser extent yaw) must have played a significant role in increasing heave and pitch loads, as they were the only two modes open for the force dissipation.

An attempt has been made to recapture this increase in the added resistance loads by adding the roll load RAOs in post-processing. The difference between the free roll plot (i.e. less built-up resistance) and the constrained roll plot is one of the important takeaways of this thesis work.

It was further observed that this constrained roll plays a very minor role in the differently heeled cases. But it is quite important when leeway is varied; especially for the 9 deg. case.

4.6. ADDED RESISTANCE INCLUDING ROLL

Salvesen method uses pitch and heave components for finding added resistance because theory was proposed for the head waves and was appropriate for that. In this thesis study, the waves are approaching from two angles of attack - leeway. So, heave and pitch are not the only dominant motions in this condition and the additional degree of freedom also need to be consider. In the case of leeway, the components of roll is added into the equation

2.5. By taking roll component into account, added resistance is increased in both the case which is about 35 percent w.r.t added resistance without roll.

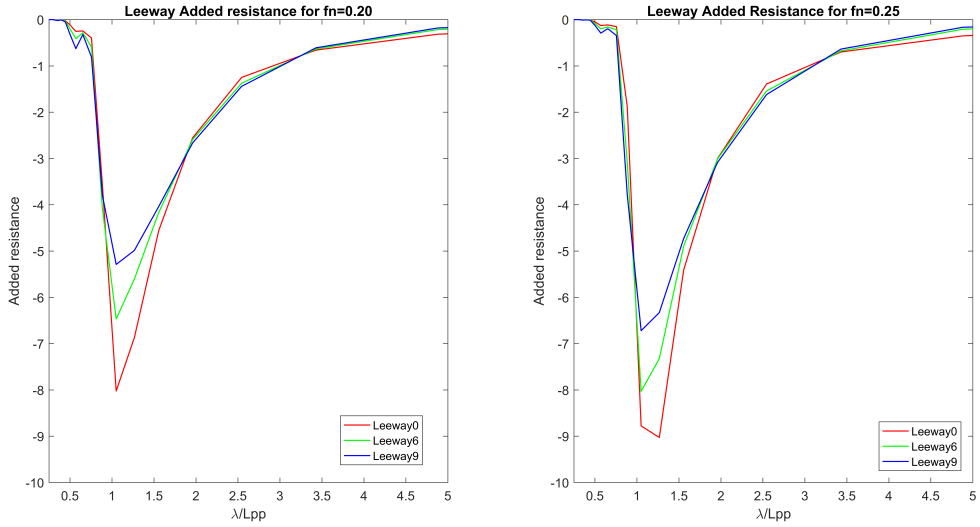

Figure 4.29: Added resistance including roll fn =0.20 and fn 0.25

4.7. CONCLUSION

In order to conclude, this chapter explains about required parameters for finding added resistance and their variations in different conditions. There is no much difference in the RAO values of heel and upright conditions but there is high a difference in RAO values of leeway conditions mainly in pitch motions. I believe this could be due to the variation in distribution of pressure around the hull and the axis it was defined. Other components like Froude krilov and diffraction force, shows there is no change in these components when compared in different conditions.

The relative vertical motion was calculated in order to show the influence of roll in leeway and the added resistance was also determined introducing roll components and not including roll components in the Salvesen equation for added resistance 2.5 . From the results, it can be seen there is about 30 percent increase in added resistance value for leeway 6 for fn = 0.20 and at fn = 0.25 it increase about 25 percent. Where as in the leeway 9 the increase in added resistance value is around 30 percent and 35 percent for fn = 0.20 and fn =0.25 respectively. In the following computed numerical results are validated with experimental results.

5

EXPERIMENTAL COMPARISON

In this section, the numerical results from the chapter 4 compared with the experimental data which was done by a master student David Markey in Tudelft towing tank [7]. As it can be seen in the following sections, the numerical results almost matches with experimental results for upright and heel condition but not in the condition of leeway. The added resistance is the second order phenomenon and predicted results are so the difference between the theory and experiment results lies between 30%-58% as stated by Salvesen [20] .

5.1. TOWING TANK

Towing tank is used to determine and investigate the hydrodynamic performance of ship and marine structures in model scale. With the help of this investigation design of the ship can be improved in the initial design or can be used for modifying the existing ship based on the requirements. The towing test relevant to the experimental type that was used in this particular case is described here.

SEMI-CAPTIVITY TEST

In semi-captivity test, the model is towed at a constant forward speed. Here the model is free to perform heave, pitch and roll motion in some cases and other motions like surge, sway and yaw are fixed. Now the added resistance shall be calculated directly by subtracting the total resistance from calm water resistance. Semi captivity test are well suited for head waves but are practically difficult to use effectively accuracy for oblique waves [9].

OVERVIEW OF EXPERIMENTAL DATA

Figure 5.1: Towing tank of Delft university of technology

5.2. UPRIGHT CONDITION

As it can be seen from the figure 5.2, high frequency and low frequency range values of added resistance are approaching zero and which correlates well with experimental results. This is due to the fact, in high frequency the occurrence of force components and motion components are low and out of phase with respect to response of the model. So, impact of the high frequency wave does not make much different on the model. In low frequency even though the force are high compare to high frequency but the motion components are in phase with the response of the model and as foresaid in the section the model will follow

the wave. The above given statement matches with the experimental results. The accuracy between numerical result and experiment can be found using this simple relation:

$$\left(\frac{Numericalvalue - Truevalue}{Truevalue}\right) * 100. \tag{5.1}$$

The true value is considered as the results obtained from the experiment. In simple the percentage determined is the difference between the numerical and experimental results. Under upright condition at fn=0.20 the difference is 6 percent for fn=0.20 and 5 percent for fn = 0.25

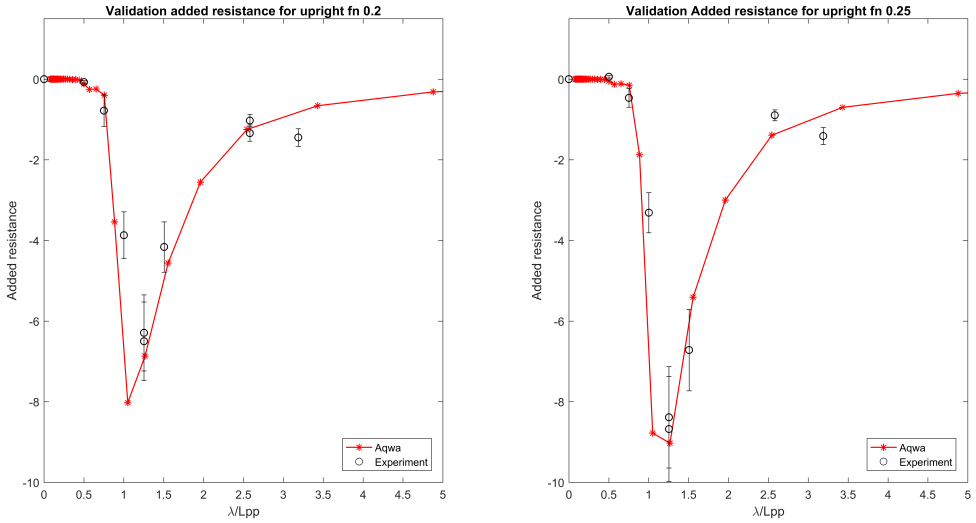

Figure 5.2: Added resistance for Upright condition fn=0.20 and 0.25

5.3. HEEL CONDITION

HEEL 10

In heel 10, the added resistance follows the same trajectory as the upright condition, but due to increase in water plane area there is also slight increase in the values of added resistance as well. Thus the difference between the experimental results and numerical results is results is minimal. But, for heel 20 condition as mentioned in section 4.1.1 influence of roll motion around $\lambda/L = 3.25$ at forward speed fn=0.20 and fn=0.25 could be seen. In case of fn=0.25, the influence further evident because of the increasing RAO values of heave as in the figure 4.2 .

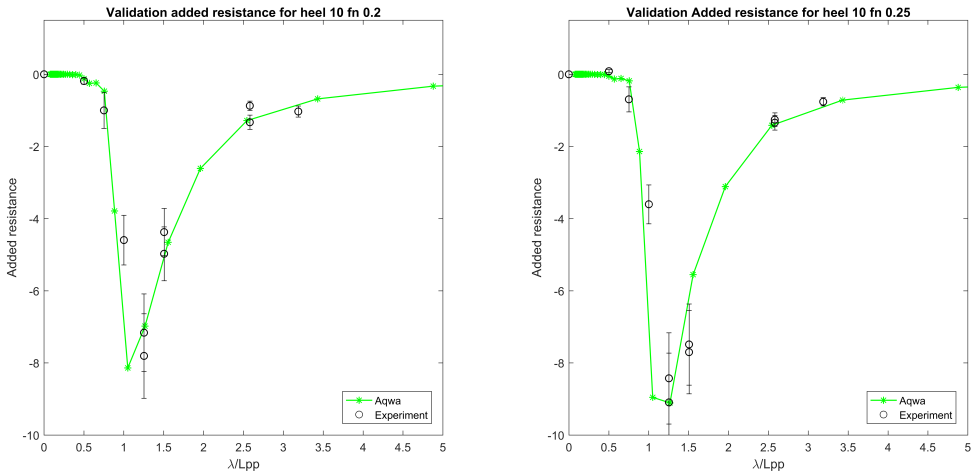

Figure 5.3: Added resistance for Heel 10 condition fn=0.20 and 0.25

HEEL20

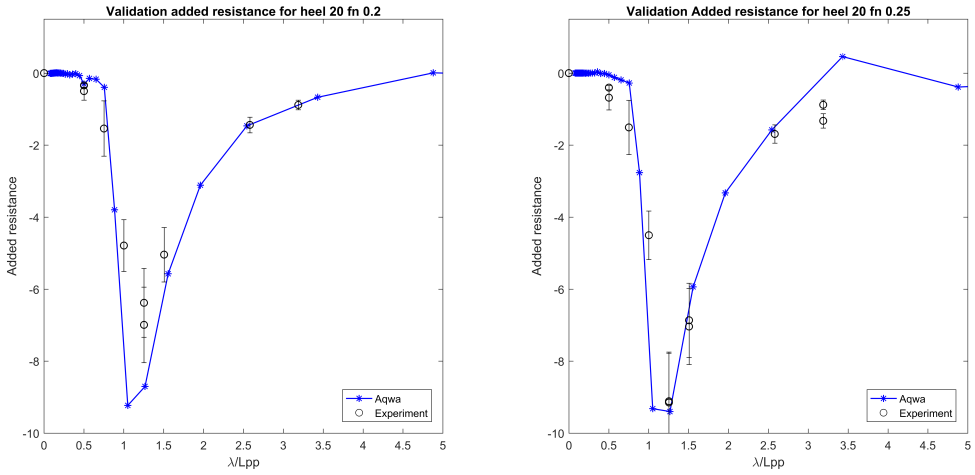

Figure 5.4: Added resistance for Heel 20 condition fn=0.20 and 0.25

5.4. LEEWAY CONDITION

5.4.1. ADDED RESISTANCE WITHOUT ROLL

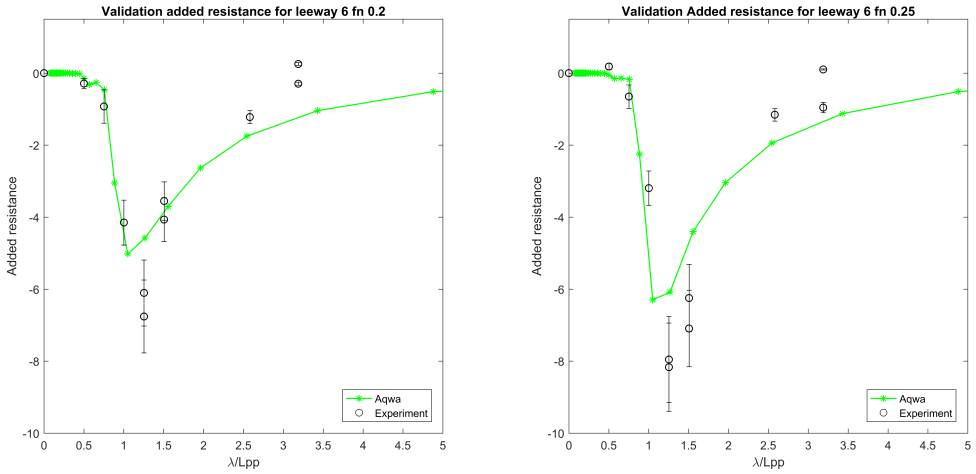

Figure 5.5: Added resistance for Leeway 6 condition fn=0.20 and 0.25

The difference between the numerical result and experimental data seems to higher than the upright and heel conditions. I believe this difference is due to the axis definition which was discussed in the section 4.5 for leeway and it's influence in pitch. Whilst, the peak value of add resistance remain around $\lambda/lpp = 1$.

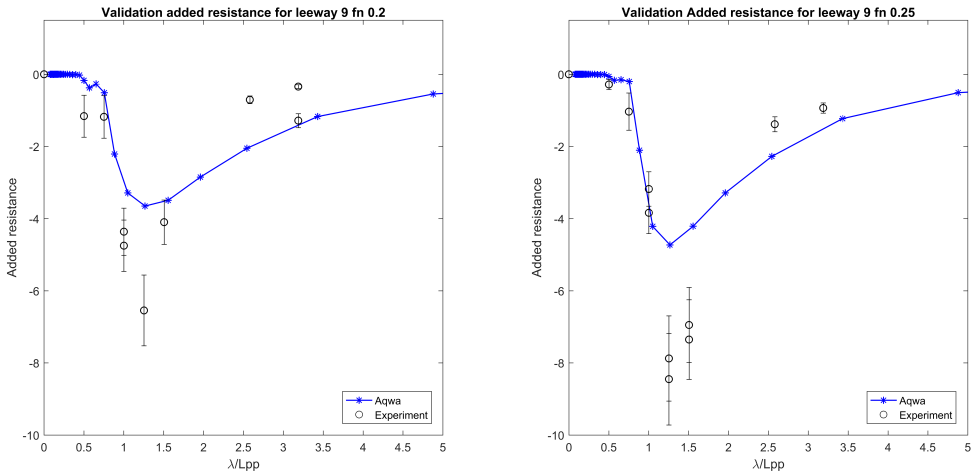

Figure 5.6: Added resistance for Leeway 9 condition fn=0.20 and 0.25

In the case of leeway 9, this the difference between the numerical results and experimental data gets even higher than leeway 6 condition. The reason for this difference is similar to limitations as stated in the previous condition and its clear that as the leeway angle increase the influence of roll as well increases

5.4.2. ADDED RESISTANCE WITH ROLL

Based on the improvement of including the proper roll components in Salvesen equation because of the angle of attack 4.6 gives the better fit with the experimental data than the condition without considering the roll. This shows the importance of roll motions in leeway.

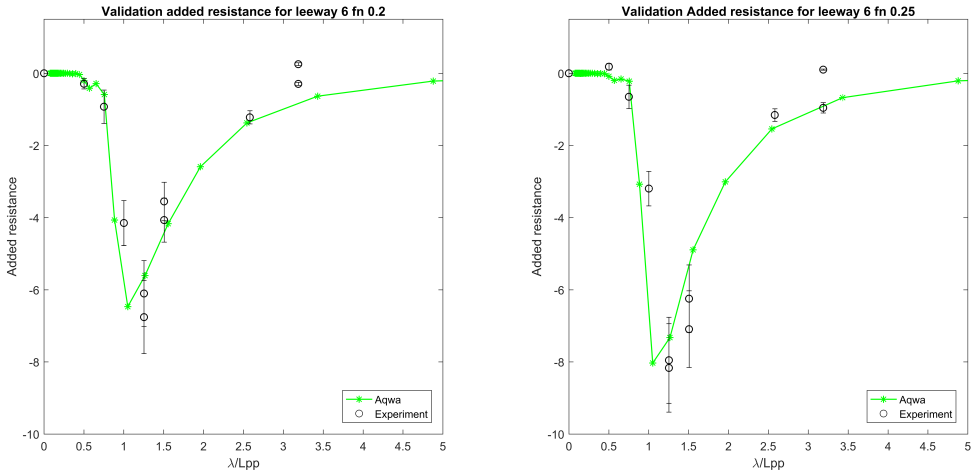

Figure 5.7: Added resistance for Leeway 6 condition fn=0.20 and 0.25

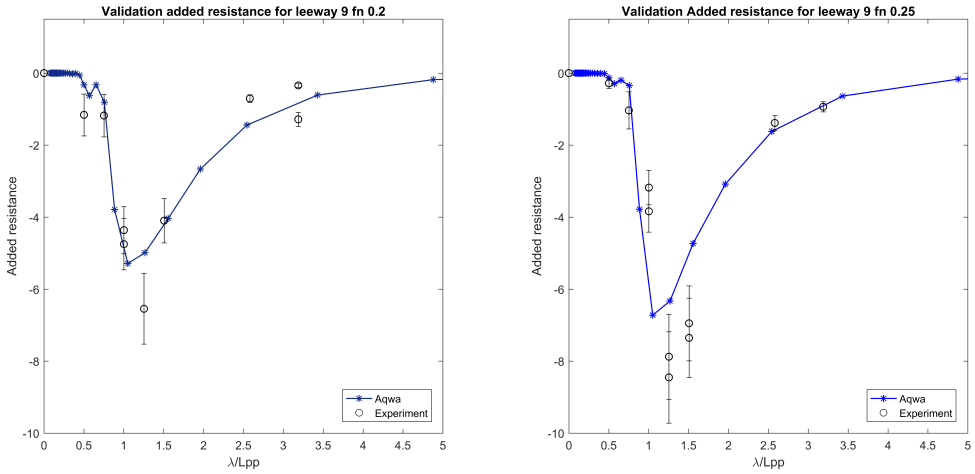

Figure 5.8: Added resistance for Leeway 9 condition f=0.20 and 0.25

5.5. RAO VALIDATION

In this section two extreme conditions of this research heel 20 and leeway 9 are chosen to validate the results.

HEAVE HEEL 20

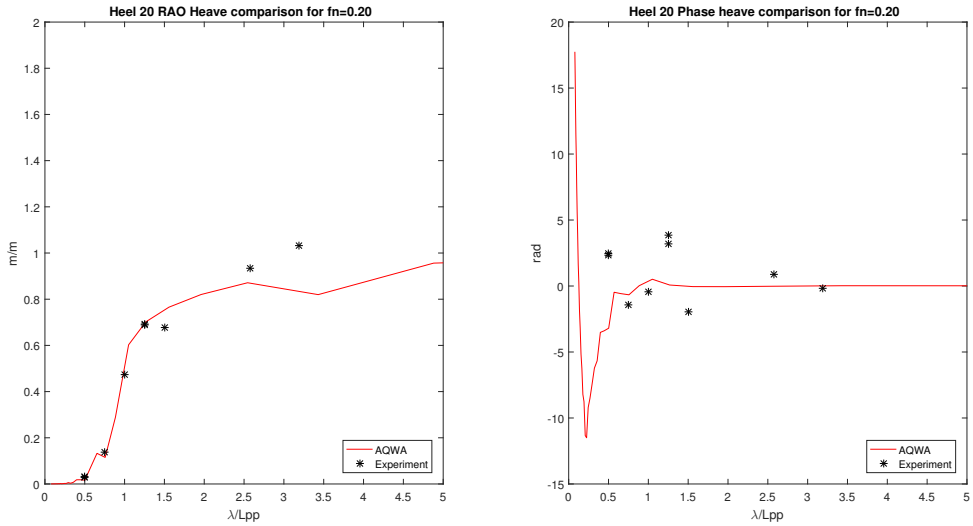

Figure 5.9: Heel 20 Heave RAO validation of ANSYS AQWA results with experimental data

From the figure 5.9, it can be seen the results align quite satisfactorily with experimental data. In high frequency, as explained in section 2.8 and as well as in low frequency the RAO values is approaching to similar to the experiment. The experiment wasn't conducted around the frequency range where the model experiences serious effects due to roll motions. So that exact conclusion can't be drawn the reason behind the sudden dip in the RAO of heel 20. Regarding the heave phase right figure 5.9, in high frequency phase is random in manner because of the wavelength is low when compared to ship length and the lag between ship reacts and incident wave varies alot and gradually this variation decreases as the frequency moves to lower frequency. In low frequency, the ship moves in phase with the waves and there wont any lag in the response which leads to zero.

PITCH HEEL 20

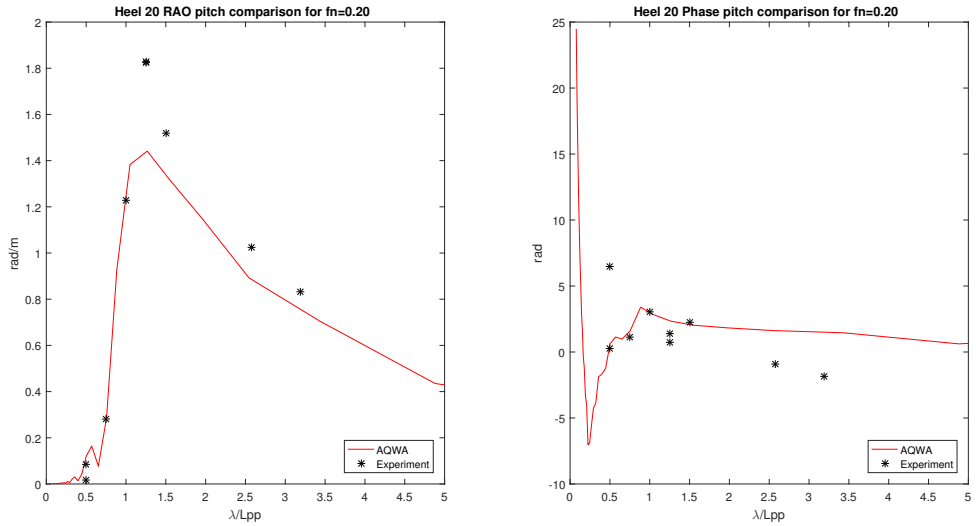

Figure 5.10: Heel 20 Pitch RAO validation ANSYS AQWA results with experimental data

From the figure 5.10, pitch RAO results almost matches with experiment data but not in the region around where the wavelength to ship length is equal to one. In pitch phase plot, the values around $\lambda/Lpp = 1$ agrees with the ANSYS AQWA results. Normally, for the pitch the phase in very long waves should approach 1.5 radians.

HEAVE LEEWAY 9

In heave condition, the experimental RAO shows the similarities with the ANSYS AQWA results but there is difference in phase graph. As said in the section how ANSYS AQWA calculates the hydrodynamic components in leeway conditions. However the difference in the RAO values of pitch with experiment is high around the intermediate frequency zone. From the validation of heel and upright conditions and the results has acceptable similarity between ANSYS AQWA and experiment. The prime reason I suspect could be restricting roll motions in leeway case. This brings me to the suggestion for alternative setup in this condition.

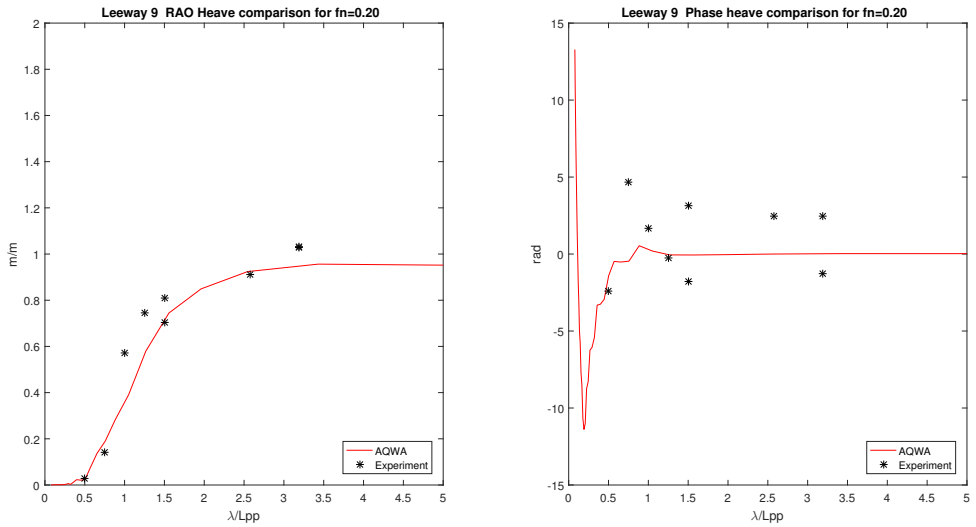

Figure 5.11: Leeway 9 Heave RAO Validation of ANSYS AQWA results with experimental data

PITCH LEEWAY 9

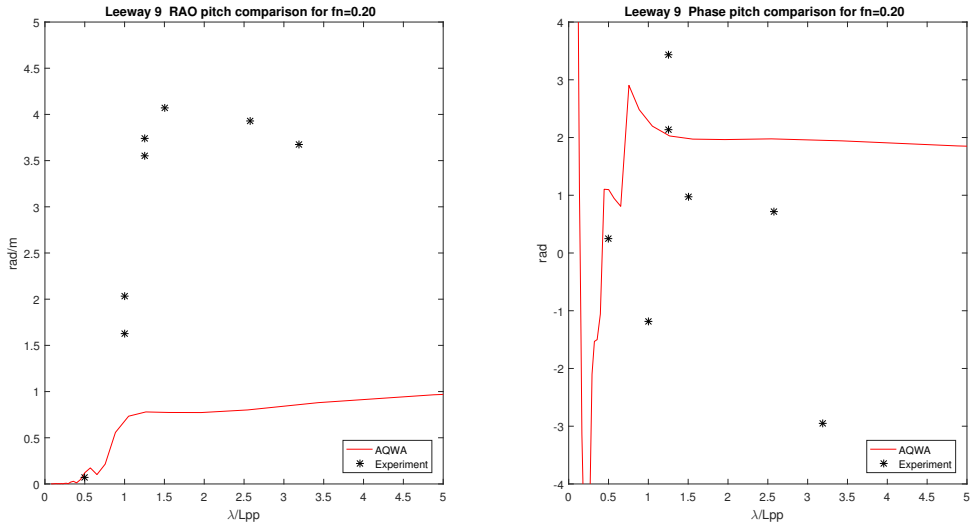

Figure 5.12: Leeway 9 Pitch RAO validation of ANSYS AQWA results with experimental data

5.6. CONCLUSION

Inorder to sum up the result found from ANSYS AQWA, the uncertainty rate for heel and leeway condition with respect to experimental data were given in percentage in table 5.1.

HEEL

Speed	Upright	Heel 10	Heel 20
fn=0.20	5.8%	-2.51%	24.5%
fn=0.25	4%	0.5%	3.12%

Table 5.1: Heel Added Resistance for fn=0.20 & fn=0.25

As you can seen from the table 5.1, the upright condition matches well with the experimental data with good accuracy and in heel conditions it can be seen that heel 10 has good accuracy with experiment for both the speeds. But the negative sign in the heel 10 (fn=0.20) states the predicted value by ANSYS AQWA is lower than the experiment. In heel 20 which is considered to extreme heel angle, due to this there will be un-balanced pressure distribution on the wetted hull surface creates a stability problem and this is will be high in lower speed [21]. I consider this could be reason, why there is high difference in the heel 20 (fn=0.20).

LEEWAY WITHOUT ROLL

Speed	Upright	Leeway 6	Leeway 9
fn=0.20	5.8%	-23%	-38%
fn=0.25	4%	-24%	-39%

Table 5.2: Leeway Added Resistance with out roll for fn =0.20 & fn=0.25

As you can seen from the table 5.2, the predicted value is low compare to the experimental value in all leeway conditions.

LEEWAY WITH ROLL

Speed	Upright	Leeway 6	Leeway 9
fn=0.20	5.8%	10 %	23%
fn=0.25	4%	8%	18%

Table 5.3: Leeway Added Resistance with roll for fn =0.20 & fn=0.25

Table 5.3 shows better correlation with experimental data than without including roll table 5.2. It can seen, neglecting roll gave the higher added resistance in the performed experiment.

5.7. ALTERNATIVE EXPERIMENTAL SETUP

5.7.1. PREVIOUS EXPERIMENTAL SETUP

In previous experimental setup, the model is kept in position by a post which behave like hinge support. The posts are placed in the front and aft of the model and each post has the transducer which capable of measuring the required hydro dynamic co-efficient as shown in figure 5.13. This setup allow only heave and pitch motions and all other motions are restricted, regardless of the position of the model. This is a very good setup for the experiment in upright condition facing head waves. However, in this case experiments are conducted in heel and leeway condition. As it became clear from the from the numerical results the influence of roll motion also plays a important role in leeway condition than heel. This leads to the another scope of this thesis proposing the alternative setup which would allow the roll motions in the experiment. Further details of the experiment can be studied from the report of D.Markey [7].

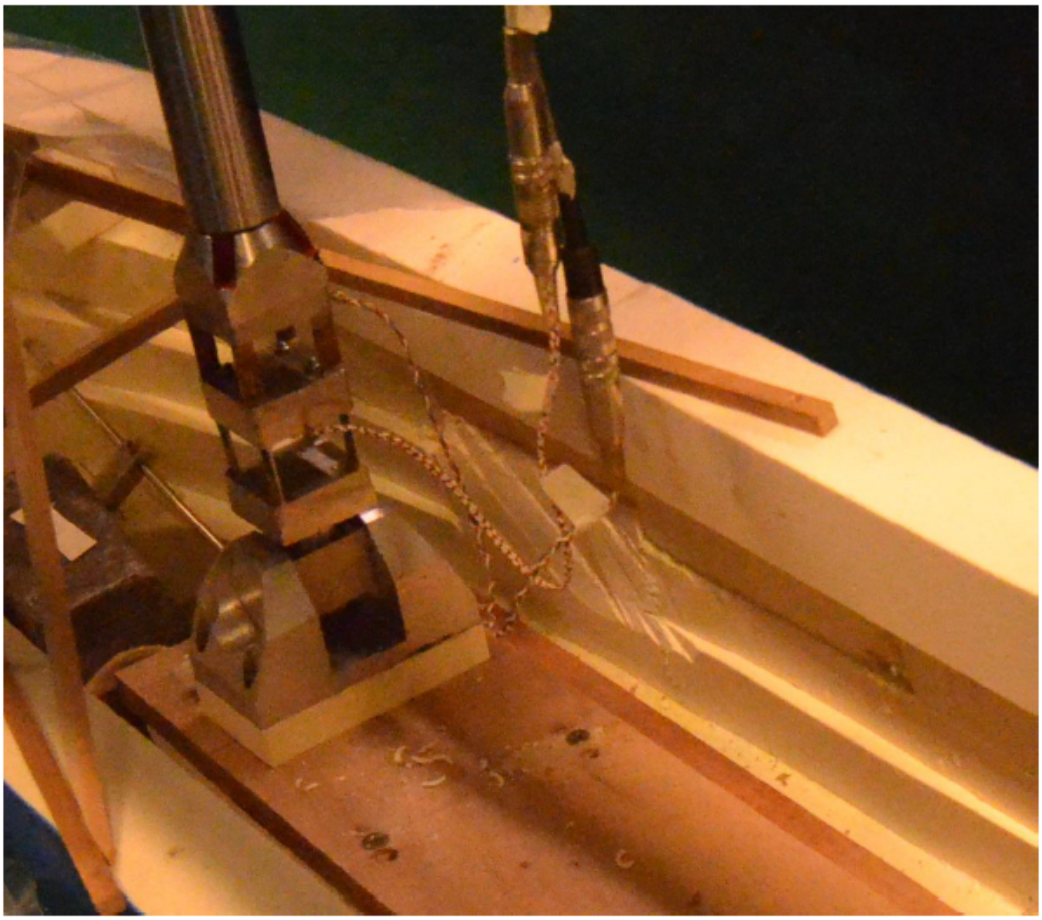

Figure 5.13: Previous experimental setup

SETUP USING SPRING

Initially, two approaches were considered for the alternative setup. One was using spring [22], which can give full freedom to move the model in all directions as shown in the figure 5.14. It can be seen that the setup seems to be complicated for the conditions like heel and leeway conditions.

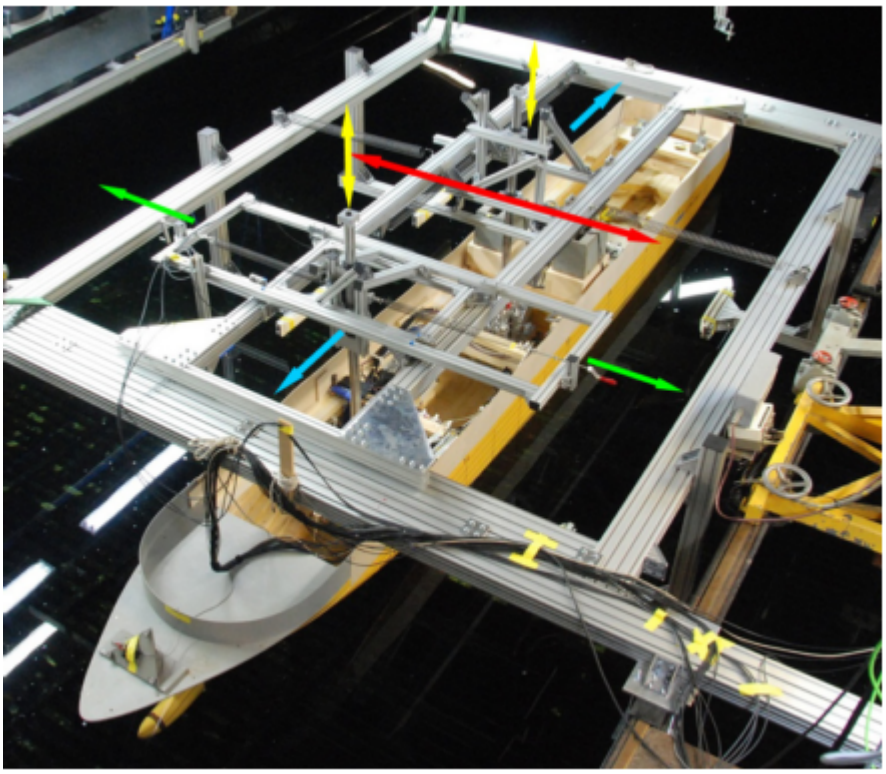

Figure 5.14: Experimental setup using spring

The stiffness of the spring varies for each degree of freedom and as well for the frequency. If the same stiffness is used through out the experiment, this may lead to some errors because the stiffness defined for one degree of freedom might restrict the other degree of freedom. To avoid this error the spring need to be changed for each condition based on the experiment needs to be carried out. It is quite a difficult setup if the type of such springs and the fact of changing them to suit the particular analysis is taken into account.

COMBINED UNIVERSAL JOINT

Considering the problems mentioned in the previous setup and as before said in the section 5.7.1 allowing roll motions along with the heave and pitch will be the main focus. For this purpose, combined universal joint is designed as shown in figure 5.15. This joint is capable of allowing translation motions (heave) and rotation (roll and pitch), if the joint is placed on the Y-axis of fixed reference axis system which is attached with rotating plate

below. Since the model is moving in the forward direction, maintaining its equilibrium is the key to the setup. Fixing the joint in lateral plane along the pivot point which is generally taken as the 1/4th of the model length from the bow. The reason why lateral plane is chosen over the longitudinal plane is because in longitudinal plane measuring heave motion require an additional spring or damper. Whereas in lateral plane with the help of this setup the sway, surge and yaw can be restricted while the remaining motions are allowed.

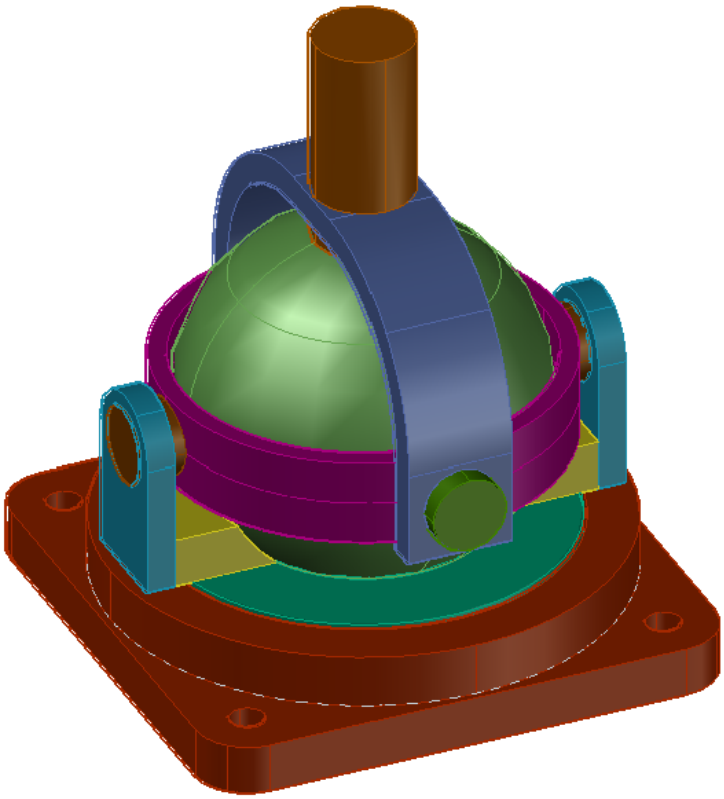

Figure 5.15: Combined universal joint

5.8. SETUP PROPOSAL

5.8.1. TYPE-I

The joint is fixed around the pivot point of the model on the both sides with the help of screw hole provided. The setup consists of ball structure which would give a smooth rotation while the rotating plate moves and clamp are attached in orthogonal direction and this

makes a combined universal joint. The rod from the joint is connected to the guiding pipe and this will be following similar mechanism like a hydraulic jack. At the end of guiding pipe, space is provided where the additional threaded rod is introduced and connected to a frame which is descendent from the carriage. This rod provides the support to the guiding pipe as well as allows roll and pitch motions. Longitudinal guiding pipe is threaded at the end and fitted with a plate to the carriage. This threading gives the free rotation along the X-axis and this helps in heave and roll motions.

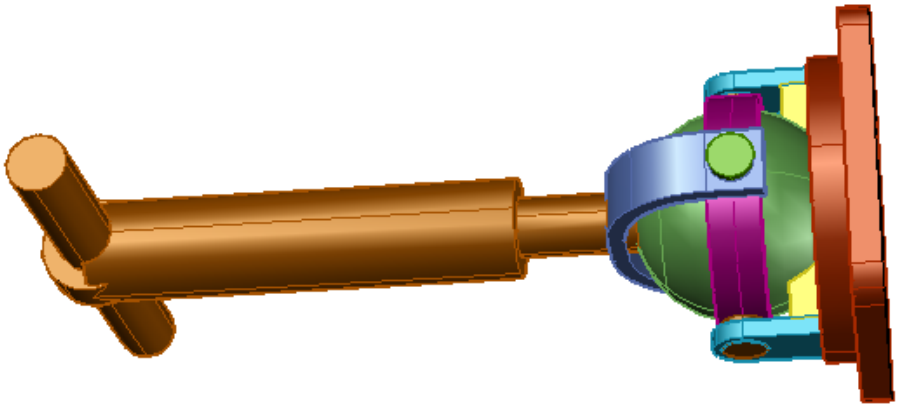

Figure 5.16: Joint end connection

However, roll, pitch and heave motion are allowed and by default surge motion is restricted from this complete setup. In order to restrict the sway and yaw, additional plate is provided on the side as show in the figure 5.17 this helps to keep the model in fixed position even at the forward speed. The sway arrest is fixed through the frame that descendent from the carriage and light weight material (like PU foam) is used considering the safety model but as well the materials need to be strong enough to resists the sway and yaw.

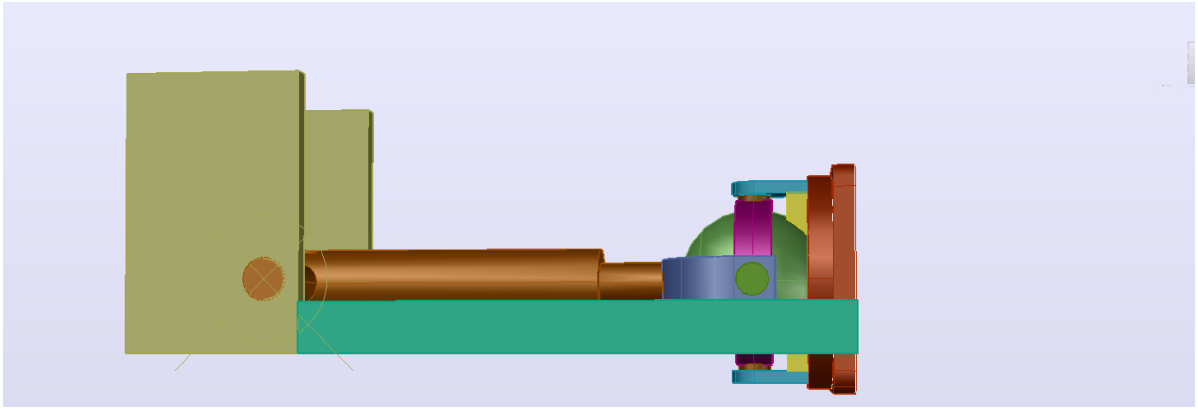

Figure 5.17: Joint with sway arrest

However, above setup meet the conditions specified for the alternative setup but placing the joint outside the model gives the clear exposure to water which might impact on the joint and causes uncertainties during the experiment. There is also a chance, when the model undergoes a motion the weight of the joint might pull them down and this would probably give unwanted inertial effects in the model results. Taking into account above mentioned factor, Type-II setup is proposed where the setup is placed inside the model. A cross-sectional view of the setup is given in the figure 5.18.

5.8.2. TYPE-II

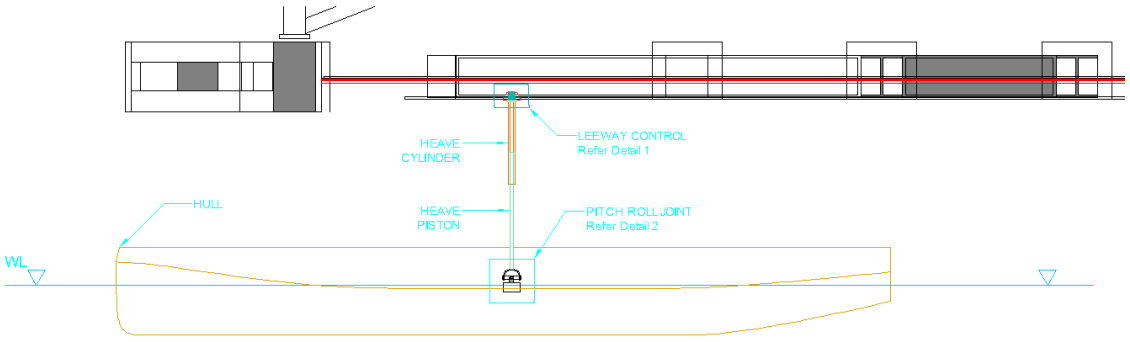

Figure 5.18: Cross section of the final setup

The two main parts of the setup, joint on the top is called as leeway control and bottom one is universal joint. The mechanism of each joint will be explained with help of figure 5.19 & 5.20.

LEEWAY CONTROL

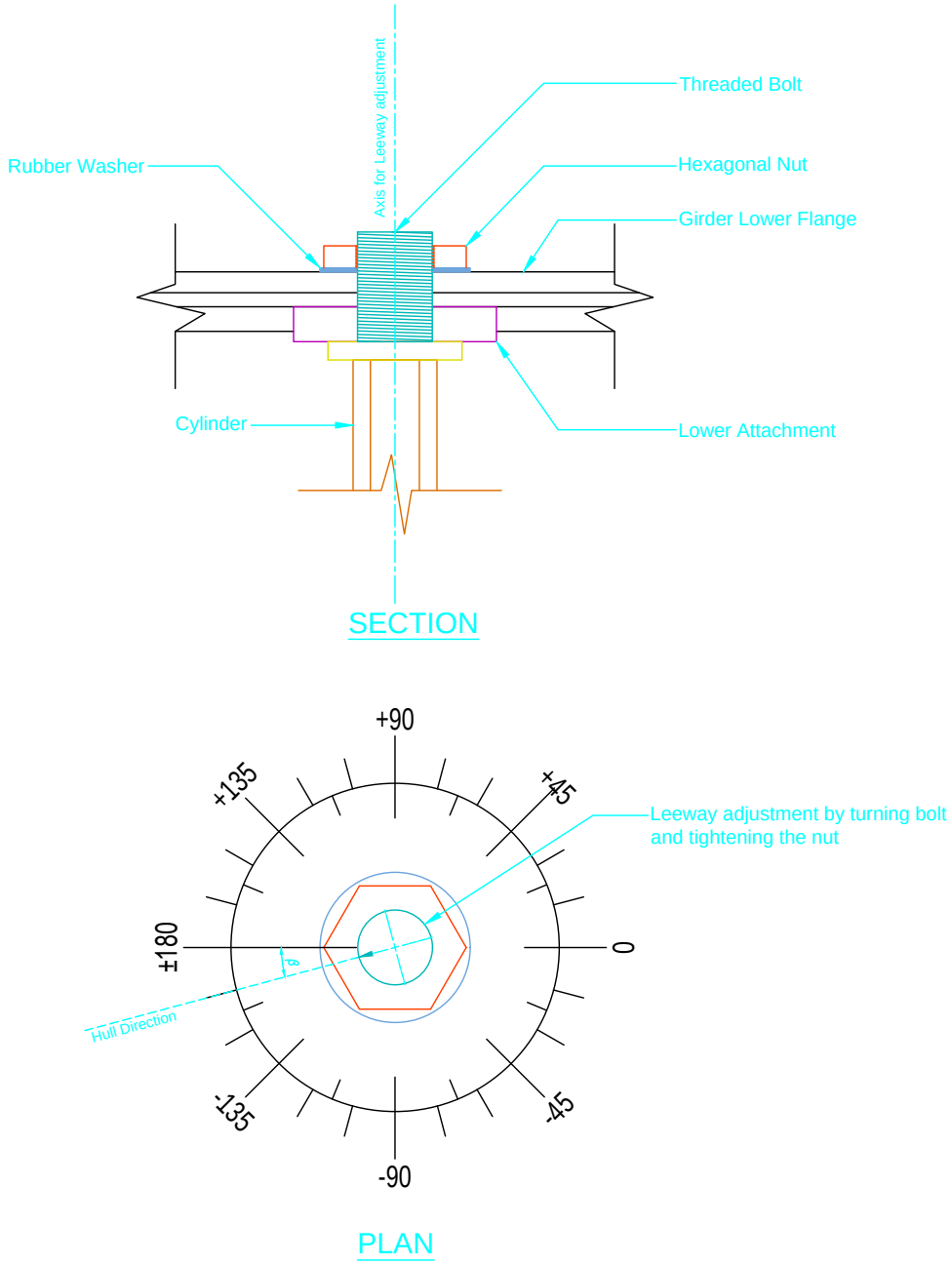

Figure 5.19: The setup to arrest yaw and sway

From the figure 5.19, the cylinder which was shown in the figure 5.13 is connected to the bolt and the threaded portion is penetrated through the carriage. Once this process is done and then the hexagonal nut which is supported by rubber washer helps to hold the model firmly in its position. A dial is attached over the nut and this dial consists of measurement of angle ranges from 0 to 180 ^{o}, to make sure the leeway angle remains the same even after the run is over. I believe this setup would be sufficient to full restrict the sway and yaw motion.

UNIVERSAL JOINT

As it can be seen in the figure 5.20, consists of two forks which connected with the help of the pin on the either side of the roll axis and pitch axis. The fork on the top provides smooth function of roll motions where as the bottom for the pitch motions. These two forks are independent to each other but however they can provide a combined motion based on the motion of the model. A shaft is provided in the center which is connected to the cylinder and by this way heave motion is also allowed. And this setup will be placed on the centre of gravity of the model same as the position where the numerical analysis should be performed to avoid unwanted coordinate axes transformations.

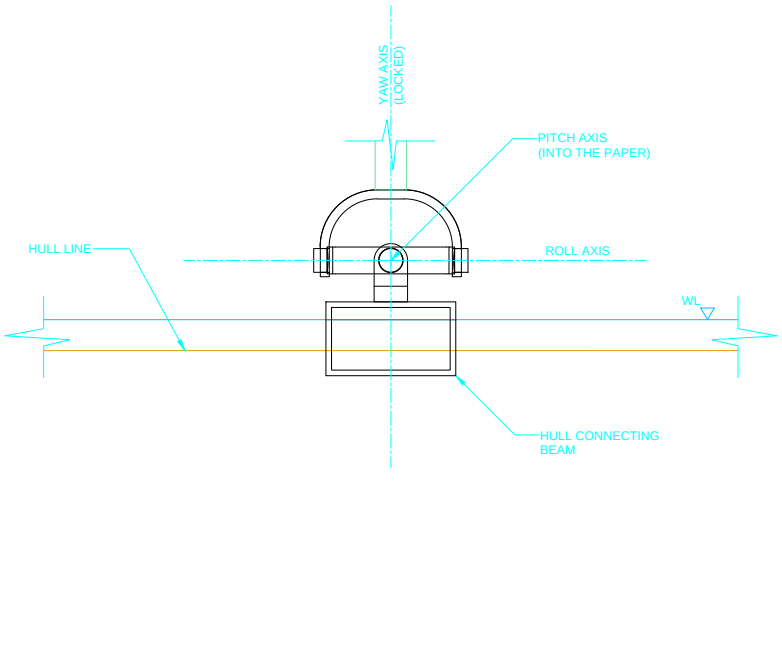

Figure 5.20: Joint allows pitch and roll

6

Conclusion and Future Recommendations

The main focus of this thesis is to predict the added resistance under the influence of two heel angles and two leeway conditions at two different forward speeds. The numerical results are validated with experimental data and based on the validated results, some recommendations are made for future investigation.

Validation and Method Choice

A 3-D potential solver (ANSYS AQWA) was used to investigate the hydrodynamic behavior of the scaled model of Ecoliner under linearized conditions. Conclusions from the past experiment [7] were very helpful in realizing that with a 2-D strip theory, important hydrodynamic effects may not be properly captured. This was also verified independently during this thesis with calculations in Seaway Octopus Office, a strip theory based program. The loss of information as opposed to AQWA was quantified and the strip theory was used for one important parameter – damping coefficients in sway and heave as inputs to the diffraction solver.

Main Numerical Analysis

The numerical results analyze variations in these three parameters: Ship upright or the effect of an initial static heel (10o and 20o taken)

- Speeds of Fn = 0.2 and Fn = 0.25 for the sailing ship
- Leeway of 6 deg and 9 deg
- Allowing or restricting free roll motions

The main purpose of this thesis emerges by analyzing these parameters: to best describe the added resistance in a numerical framework. Added resistance shows up as efficiency lost for a propelling ship, hence a broad study of optimizing the parameter is highly desirable.

ROLL EFFECT

It is seen from the analyses that the numerical added resistance is about 20 to 25% different (lower) from the results of the background experiment performed [7]. This is with a good description of the roll-direction loads which were restricted in the experimental setup. Allowing free roll motion increases the difference to about 40 to 45%. This helps in properly understanding the significance of restricting roll and the high increase in added resistance it causes.

LEEWAY EFFECT

The effect of leeway in reducing added resistance felt by the ship is very positive. This table briefly summarizes for the higher Fn = 0.25 speed with the roll restraint properly considered:

Leeway	Added resistance reduction
0	Base case
6	About 11 % reduced
9	About 25 % reduced

Table 6.1: Added resistance reduction in Leeway

It is a strong indication that especially for higher speeds, using a fairly high leeway to sail would offer massive advantages in reducing the resistance. Thus, it improves fuel cost and sustainability.

The other effects like heel and the sailing speed, by itself, are not that interesting in resistance reduction. It is strongly advised to focus research efforts towards better understanding the leeway. The idea is to try and find an optimal combination of maintaining a heading that is the most productive as well as sailing the Ecoliner with the proper course.

COMMENT ON PARAMETER SENSITIVITY

As the previous part noted, leeway is the most sensitive and interesting parameter. The benefit offered to the ship seems to scale quadratically as the leeway angle is increased.

Better description of roll behavior would also be helpful.

A limitation of this thesis is that just like the experiment which this work is based on, the effect of the yaw restraint remains largely unknown. The author of [] noted that because of the model setup there was high uncertainty and poor repeatability in the side force and yaw moment modelled. To be careful, within this analytical exercise, only the roll loads were used to study resistance results.

Because this unknown factor about the yaw persists, there is a chance that greater benefits may be derived than what are documented here. It is quite difficult to quantify this effect without further experimental work in this specific area.

RECOMMENDATIONS FOR FURTHER WORK

The work done in this thesis made clear that a few potential follow-up topics could be investigated.

First, an important finding about the previous experimental effort need to be mentioned which became extremely clear after analyzing and processing data during this thesis. To try and model a system in the towing tank which only allows for heave and pitch while completely restricting all the other four modes is strongly discouraged. The reason is simply practical. To visualize such a system setup would would have to use considerably complex mechanical interfaces. That makes trying to register, and more importantly, to translate any measured data (for example with a set of transducers) more challenging and prone to errors.

It is advised to set a system up which complete restrains the three horizontal motions but allow heave, roll and pitch without issues. Logical next step is to then try and describe the roll behavior well in an analytical framework, account for it and arrive at a heave-and-pitch-only added resistance.

A couple of experimental set ups have been proposed. Of these, the type II as described in 5.18 with a leeway control and universal joint is seen as the more promising one.

It will be quite fascinating to follow-through with possibly higher leeway angles and see at what limit it stops being a benefit for the transit. To conclude, analytical work plus experiments there could help to optimize the three factors of adequate sailing stability (sails),

good hydrodynamic behaviour (hull) and the most efficient sailing leeway for the Ecoliner's transport.

It would be interesting to carry out the experiment combining both heel and leeway and find out how the model would behave.

The literature [23], states that as the leeway angle increases, the generation of vortex on the leeward side also increases.This influence of vortex on the added resistance deserves to be investigated.

BIBLIOGRAPHY

[1] D. Prasanna, *The ship's motions at sea,* https://hubpages.com/travel/theshipsmotionsatsea.

[2] J. Journee and W. Massie, *Offshore hydromechanics,* (2001).

[3] J. Blok, *J.J. Blok,The Reistance Increase of a ship in waves,* .

[4] K. Ouchi, K. Uzawa, A. Kanai, and M. Katori, *Wind Challenger the Next Generation Hybrid Sailing Vessel,* (2013).

[5] B. Guo, *Numerical and Experimental Investigation of Added resistance in waves,* (2011).

[6] H. Yihuai, T. Juanjuan, X. Shuye, and L. Shewen, *Stability criterion and its calculation for sail-assisted ship,* (2015).

[7] D.J.Markey, *Influence of heel and leeway on added resistance in waves,* (2013).

[8] LeoH.Holthuijsen, *Waves in oceanic and coastal waters,* (2007).

[9] R. Grin, *on the Prediction of Wave Added Resistance With Empirical Methods,* (2012).

[10] L. Bergdahl, *Wave-Induced Loads and Ship Motions,* (2009).

[11] J. Journée, *Quick strip theory calculations in ship design,* (1992).

[12] J. Gerritsma and W. Beukelman, *Analysis of the resistance increase in the waves of the fast cargo ship,* (1972).

[13] H. Zeraatgar and F. Abed, *Added resistance and Drift force analysis in regular and irregular waves,* (2006).

[14] J. M. J. Journée and L. J. M. Adegeest, *Theoretical Manual of Strip Theory Program Seaway for Windows* , (2003).

[15] I. Journee, *Strip theory algorithms,* (1988).

[16] H. Liang, Z. Ren-chuan, M. Guo-ping, and F. Ju, *Study on Havelock form translating-pulsating source Green's function distributing on horizontal line segments and its applications,* (2016).

[17] ANSYS Inc., *ANSYS AQWA Theory Manual,* (2013).

[18] R. Datta, N. Fonseca, and C. Guedes Sorares, *Analysis of the forward speed effects on the radiation forces on fast ferry,* (2013).

[19] C. Liaw and S. Bishop, *Nonlinear heave-roll coupling and ship rolling,* (1993).

[20] N. Salvesen, E. Tuck, and Faltinsen, *Ship motions and sea loads,* (1970).

[21] A. S. Darvazehoie, *Stability of ships with forward speed,* (1989).

[22] P. Valanto and Y. Hong, *Experimental Investigation on Ship Wave Added Resistance in Regular Head , Oblique , Beam , and Following Waves,* (2015).

[23] W. Bradbury, *An experimental investigation of the flow past hulls at leeway,* (1985).